Journal of Microbiological Methods 163 (2019) 105656

Contents lists available at ScienceDirect

Journal of Microbiological Methods

journal homepage: www.elsevier.com/locate/jmicmeth

Review

Algae-based metallic nanoparticles: Synthesis, characterization and applications

Prerna Khanna, Amrit Kaur, Dinesh Goyal*

Department of Biotechnology, Thapar Institute of Engineering and Technology, Deemed University, Patiala 147 004, Punjab, India

ARTICLE INFO

Keywords:
Nanoparticles
algae
green chemistry
microbial synthesis
physicochemical properties

ABSTRACT

Nanomaterials (NMs) tailored *via* conventional physicochemical routes play havoc with the environment that has led to the evolution of competent green routes for the actualization of a circular economy on an industrial-scale. Algae belonging to the class *Cyanophyceae, Chlorophyceae, Phaeophyceae* and *Rhodophyceae* have been harnessed as nano-machineries through intracellular and extracellular synthesis of gold (Au), silver (Ag) and several other metallic nanoparticles. Algae are an appealing platform for the production of diverse NMs, primarily due to the presence of bioactive compounds such as pigments and antioxidants in their cell extracts that act as biocompatible reductants. *Chlorella* spp. and *Sargassum* spp. have been extensively explored for the synthesis of nanoparticles having antimicrobial properties, which can potentially substitute conventional antibiotics. Characterization of nanoparticles (NPs) synthesised from algae has been done using advanced spectroscopic, diffractographic and microscopic techniques such as UV-Vis FT-IR, DLS, XPS, XRD, SEM, TEM, AFM, HR-TEM, and EDAX. The present paper reviews the information available on algae-mediated biosynthesis of various NPs, their characterization and applications in different domains.

1. Introduction

Synergy between engineering and medical sciences has opened novel frontiers in the ever-growing new domain of nanotechnology aimed at genesis, implementation and use of nanomaterials (NMs) to integrate with biological research. The fountainhead of nano-biotechnology is the fabrication of nanoscale particles by virtue of biological moieties that influence the characteristics of nanoparticles (NPs). Synthesis of NMs of diverse sizes and shapes has underpinned great interest due to their novel properties as compared to their bulk counterparts. Consistency in the chemical, biochemical and physicochemical properties of materials varies immensely at the nanoscale mainly due to the high aspect ratio of surface area to volume. This leads to considerable differences in biological and catalytic activity, mechanical properties, melting point, optical absorption, thermal and electrical conductivity (Shah et al., 2015). Nanoparticles bridge the gap between bulk materials and atomic or molecular structures. Physicochemical synthesis of NPs is often cumbersome and costly with the release of harmful by-products posing a high risk to living systems (Sinha et al., 2009; Azizi et al., 2014). Biological synthesis of NPs using microbes, enzymes, plants, and algae has been proposed as an alternative to chemical and physical modes of synthesis. The prime focus is on selecting the compounds which are competent, harmless, eco-friendly and commercially viable. In the past few years, phyconanotechnology, though in its stage of infancy, is becoming an exciting and upcoming area with greater scope in the synthesis of algae-based NPs. Algae being the largest photoautotrophic group of microorganisms are the potential source for an array of secondary metabolites, pigments and proteins, which can serve as nanobiofactories for metallic nanoparticles (Ali et al., 2011; Prasad and Elumalai, 2013; Namvar et al., 2015; Aziz et al., 2015; Kalabegishvili et al., 2012; Patel et al., 2015; González-Ballesteros et al., 2017).

Simple methods have been developed comprising of extracellular or intracellular reduction of metal ions by biological extracts (Li et al., 2011; Roychoudhury and Pal, 2014; Parial and Pal, 2014). Extracts from plants (Sangeetha et al., 2011), bacteria (Li et al., 2011), fungi (Mukherjee et al., 2002), human cells (Anshup et al., 2005; El-Said et al., 2014) and diatoms (Schröfel et al., 2011) have successfully transformed metal precursors to their corresponding NPs. The synthesis of these NPs has been facilitated by a soup of compounds such as terpenoids, phenolics, flavonones, amines, amides, proteins, pigments, alkaloids etc., present in the extracts, which assists in metal reduction and their stabilization (Asmathunisha and Kathiresan, 2013). The high metal uptake potential of algae and their predominance makes them a low-cost raw material (Kannan et al., 2013a). The interaction and biochemical activities of every microbe and the internal factors such as

* Corresponding author.
E-mail address: dgoyal@thapar.edu (D. Goyal).

https://doi.org/10.1016/j.mimet.2019.105656
Received 26 September 2018; Received in revised form 14 June 2019
Available online 17 June 2019

pH and temperature eventually play a crucial role in the size and morphology of the NPs (Makarov et al., 2014; Shah et al., 2015; Pathak et al., 2019). The high surface area to volume ratio justifies their versatile applicability together with their ability to withstand harsh conditions (Dahoumane et al., 2016). Their synthesis plays a vital role due to their broad spectrum applications, which diverge from medical, industrial, electronic devices, sensors, cosmetics, pharmaceutical, agriculture and bioremediation.

The present paper comprehensively reviews work done on algae-mediated biosynthesis of gold (Au), silver (Ag), palladium (Pd), platinum (Pt), iron (Fe), cadmium (Cd), titanium oxide (TiO_2), zinc oxide (ZnO) and Ag-Au bimetallic nanoparticles and their mechanism of synthesis followed by advances in characterization techniques with their application in different domains.

2. Classification of nanoparticles

A wide range of NPs exists naturally in the environment or can be fabricated artificially; the latter is sometimes called anthropogenic NPs. Despite the presence of natural NPs in living organisms, their existence is assumed in the biosphere since the genesis of the earth. Natural NPs can be obtained as a result of forest fires, volcanic eruptions, weathering of rocks, explosion of clay minerals, soil erosions, and sandstorms (Baker et al., 2013). NPs are classified in different categories based on shape and dimension, phase composition and nature of the material (Fig. 1).

3. Synthesis and characterization of nanoparticles

Fundamentally there are two approaches for the synthesis of NPs, the top-down approach and the bottom-up approach). The top-down approach involves slicing of bulk materials into reduced size self-assembled nanoscale objects. It often uses microfabrication techniques, where externally controlled tools are used to cut, mill, and shape materials into the desired size and shape (Nath and Banerjee, 2013; Khan et al., 2017). A variety of metallic NPs were fabricated by top-down approaches like mechanical milling (Arbain et al., 2011), etching (Cheng et al., 2016), laser ablation (Amendola and Meneghetti, 2009), sputtering (Hatakeyama et al., 2011) and electro-explosion (Ghorbani, 2014). Whereas the bottom-up approach is reversed altogether therefore referred to as molecular nanotechnology involving assembly of a defined structure by joining atom by atom, molecule by molecule, cluster by cluster or self-organization (Thakkar et al., 2010). In this mode, self-assembled properties of single molecules are exploited to build up complex conformations at the nanoscale (Nath and Banerjee, 2013). Nanoscale structures that have been reported to be synthesised by bottom up approaches are supercritical fluid synthesis (Türk and Erkey, 2018), use of templates (Apolinário et al., 2014), plasma or frame spraying synthesis (Tanaka, 2018.) sol-gel process (Sekine et al., 2009), laser pyrolysis (D'Amato et al., 2013), chemical vapour deposition (Bhaviripudi et al., 2010), molecular condensation (Gurentsov et al., 2007), chemical reduction (Guzmán et al., 2009) and most significantly green synthesis (Sangeetha et al., 2011; González-Ballesteros et al., 2017) (Fig. 2). The main focus is inclined towards synthesis of NPs of different chemical composition, sizes, morphologies and monodispersity (Sastry et al., 2003; Iravani, 2011).

In top-down approaches, physicochemical processes are involved which may lead to surface imperfections that affect the NPs properties. Similarly, in bottom-up approaches, NPs are clustered from smaller units. So in both cases, the growth of the NPs is controlled *via* kinetic processes which determine the shape and size of the NPs. The energy and growth rate of crystals are monitored by introducing compatible templates or surfactants which can curtail the interfacial energy (Sharma et al., 2011; Khan et al., 2017). There is an array of various

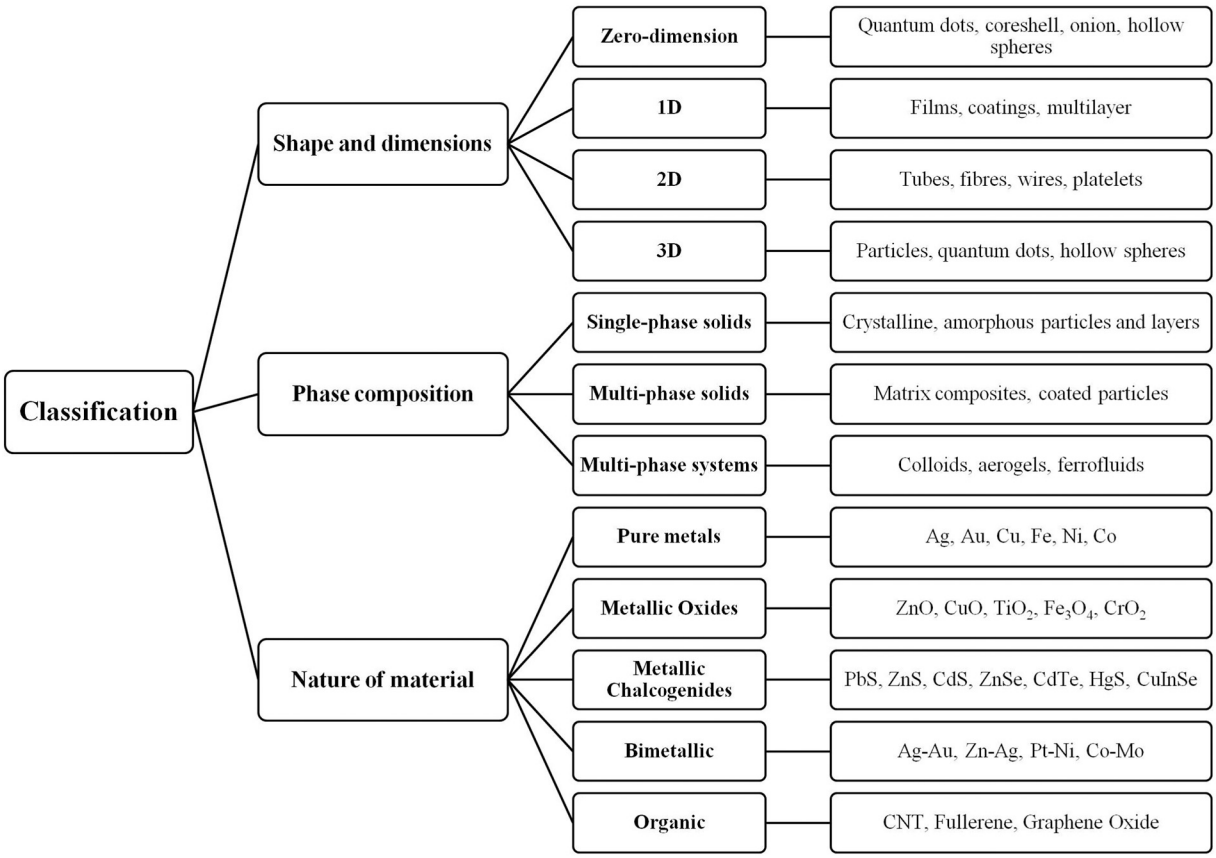

Fig. 1. Classification of nanomaterials (NMs).

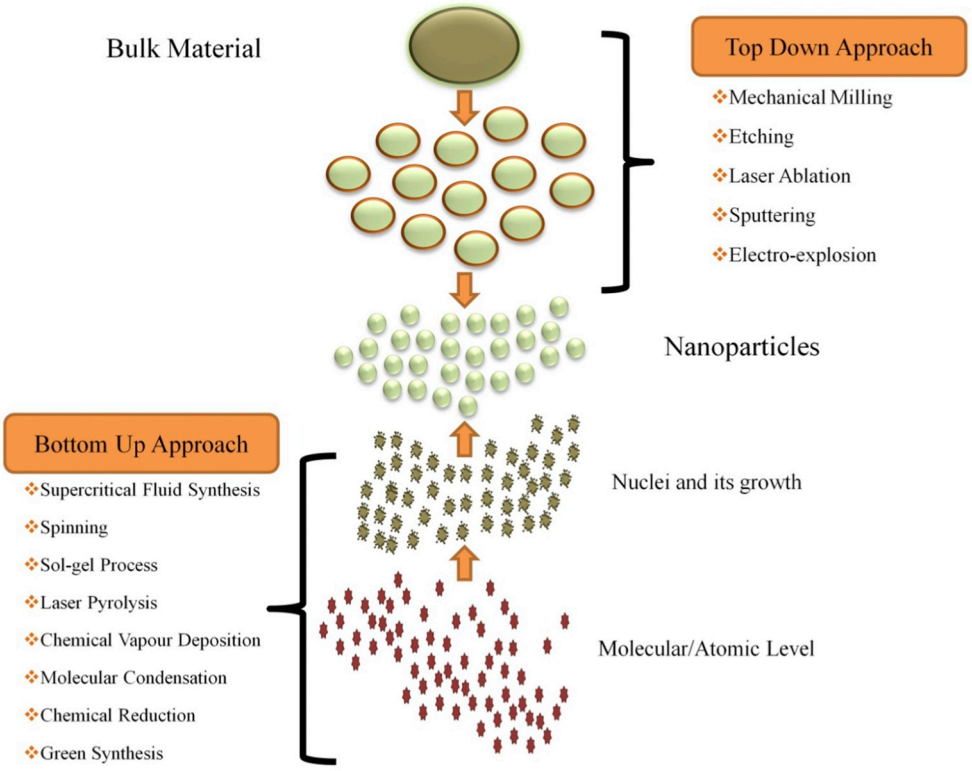

Fig. 2. Synthesis of nanomaterials (NPs) *via* top-down and bottom-up approaches.

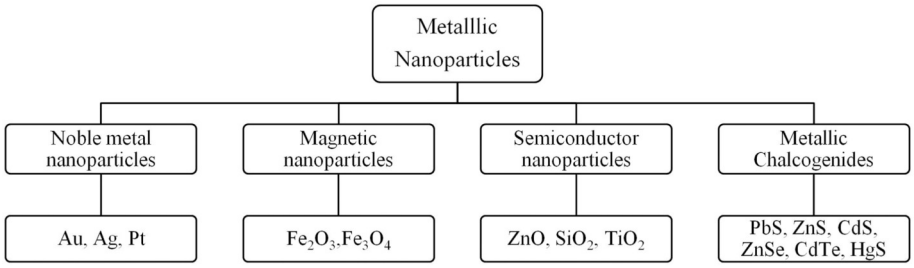

Fig. 3. Different types of metallic nanomaterials (NPs).

kinds of metallic NPs depending on their metallic behaviour, magnetic properties etc. (Fig. 3). Up until now, various commercial surfactants such as cetyl trimethyl ammonium bromide (CTAB), polyvinylpyrrolidone (PVP), sodium dodecyl sulfate (SDS), thioglycerol (TG), mercaptoethanol (ME), sodium hexametaphosphate (SHMP) (Rahdar, 2013) have been used as capping agents, which could directly modify the surface morphology of NPs during their synthesis. Usually, a colour change is the convenient visible signature and the qualitative indication for any reaction to take place in the biological/chemical synthetic process. Most of the NPs are fabricated in a colloidal solution which can be detected easily (Poinern, 2014; Khan et al., 2017). After completion of the reaction, the NPs are subjected to simple downstream processing such as high-speed centrifugation for their recovery (Poinern, 2014).

Thereafter, NPs are subjected to various characterization techniques to ascertain their size, shape, distribution, surface morphology, and surface area. Spectroscopic and diffractographic techniques involved in the characterization include UV-visible spectroscopy (UV-vis), dynamic lights scattering (DLS), energy dispersive spectroscopy (EDS), X-ray diffraction (XRD), Fourier transform infrared spectroscopy (FT-IR), X-ray photo-electron spectroscopy (XPS) and Raman spectroscopy (Menon et al., 2017; Shah et al., 2015). These are the indirect methods used to analyse composition, structure, and crystal phase. Whereas scanning electron microscopy (SEM), transmission electron microscopy (TEM), high-resolution transmission electron microscopy (HR-TEM), and atomic force microscopy (AFM) are employed to determine the size and morphological features of NPs (Quester et al., 2013; Hulkoti and Taranath, 2014).

3.1. Spectroscopic and diffractographic techniques

Generally, metallic NPs have striking optical properties due to surface plasmon resonance (SPR), which is monitored by UV-Vis spectroscopy within the range of 190–1100 nm (Sharma et al., 2016). These radiations interact with the metals and promote the electronic transition from ground to higher energy state and a specific SPR band is obtained which may help to obtain the size and shape of NPs up to a certain limit (2–100 nm) (Poinern, 2014). The absorption spectra for different materials is different e.g. for Ag-NPs it is 400–450 nm (Verma et al., 2010; Aboelfetoh et al., 2017), for Au-NPs it falls in between 500–550 nm and for ZnO-NPs it is between 350 and 390 nm (Poinern, 2014; Shukla and Iravani, 2017).

It has been suggested that the broadening of the SPR band width, which illustrates a shift toward the red or blue end is considered as an

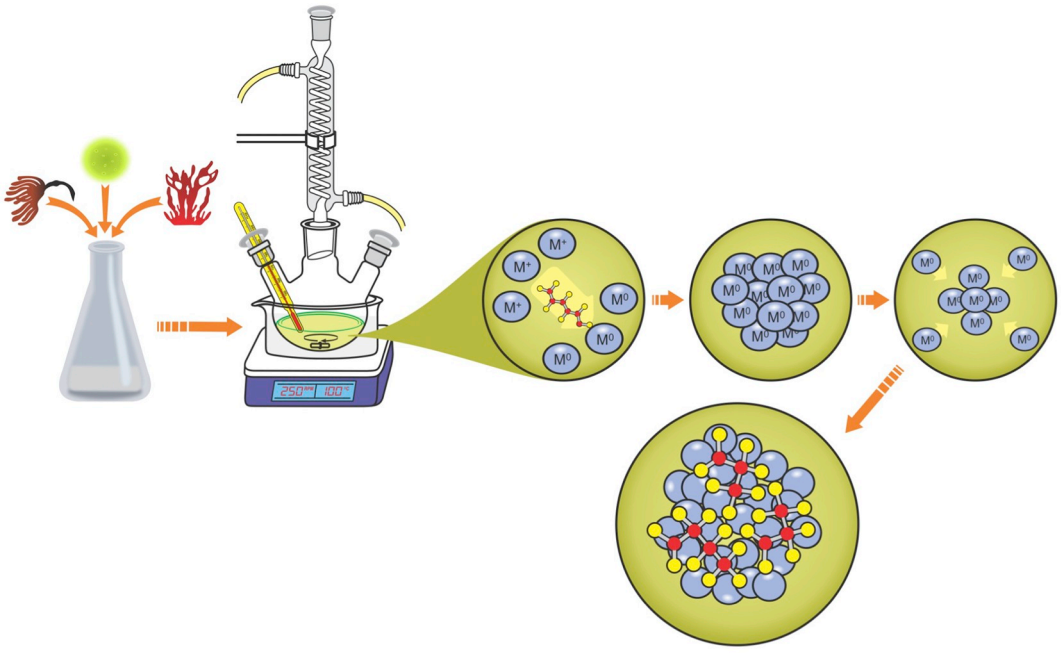

Fig. 4. Mechansim of synthesis of nanomaterials (NPs) from algae.

index of size, state of aggregation, shape, the type of capping or binding agents, polydispersity, and the surrounding dielectric medium (Govindaraju et al., 2008; Jena et al., 2013, Mahmudin et al., 2015). Furthermore, an increase in particle size in the aqueous solution is depicted by an increase in band intensity. UV/Vis- diffuse reflectance spectrometer (DRS) is a fully equipped device, which can be used to measure the optical absorption, transmittance and reflectance. DRS is an exceptional technique to calculate the bandgaps of NMs which is important for determining the photoactivity and conductance of the material (Khan et al., 2017; Shukla and Iravani, 2017).

To investigate the underlying mechanism of synthesis and surface chemistry, FT-IR spectroscopy is done to identify the functional groups attached to the NPs. Usually, it ranges between 4000 and 400 cm^{-1}, and a resolution of 4 cm^{-1} gives a clear idea about the reducing agents responsible for capping, reduction and stabilization. The comparison between the transmittance spectra of aqueous native extract and reaction medium gives an idea of the biomolecules involved in the process (Dahoumane et al., 2016). Most common functional groups, which adhere to the NPs are −C=O−, $-NH_2-$ and −SH− (Jena et al., 2013, 2014). However, FT-IR has limitations because of the high degree of overlapping of IR absorption bands in the complex biological matrix. Additionally, other characterization techniques, such as XPS, could shed light on the interaction between the produced NPs and their surrounding biomolecules (Dahoumane et al., 2016).

Surface charge, hydrodynamic diameter and distribution of NPs in liquid form is measured by DLS spectroscopy and particle stability is determined by zeta potential (Poinern, 2014). Whereas the purity, crystalline size, geometry, orientation and phases can be determined by XRD data, generally the diffraction patterns are compared with the standard crystallographic database like JCPDS to have the structural information (Shah et al., 2015). It gives a rough idea about the particle size determined by Debye Scherer formula (Ullah et al., 2017). XRD works well with both single and multiphase identification of NPs. Moreover, XRD diffractogram gets influenced with amorphous NMs having varied inter-atomic lengths (Ingham, 2015).

3.2. Advanced microscopic techniques

Properties of NPs are greatly influenced by their morphology which is studied by advanced microscopic techniques such as SEM, TEM, AFM and HR-TEM. SEM provides information about particles at the nanoscale and assists in determining the surface morphology and dispersion of NPs in bulk or matrix. TEM is most commonly used for size and shape, and it can also provide information about the number of material layers as it varies from low to high magnification. However when both are combined with EDAX or EDS, information is given about the metals present (Oza et al., 2012). In some cases of intracellular synthesis of NPs, localization of synthesized NPs is explored by SEM and TEM. However, in order to determine the exact shape, size and crystalline structure HR-TEM is absolutely required. AFM on the other hand provides information on surface topography. While TEM images mainly represent a two-dimensional image of three-dimensional nanoparticles, AFM can be used to obtain three-dimensional information of synthesized particles (Quester et al., 2013; Khan et al., 2017).

4. Mechanism of synthesis of nanoparticles from algae

Algae are known to hyperaccumulate heavy metal ions and possess an exceptional capability to remodel them into more malleable forms (Fawcett et al., 2017). Because of these alluring attributes, algae have been foreseen as model organisms for fabricating bio-nanomaterials. Algal extracts consist of carbohydrates, proteins, minerals, oil, fats, polyunsaturated fatty acids along with the soup of bioactive compounds such as antioxidants (polyphenols, tocopherols), and pigments such as carotenoids (carotene, xanthophyll), chlorophylls, and phycobilins (phycocyanin, phycoerythrin) (Michalak and Chojnacka, 2015). These potentially active compounds have been elucidated as reducing and stabilizing agents (Fig. 4). From the available reports, algae-mediated synthesis of NMs involves preparation of (i) algal extract, (ii) metal precursor solution, and (iii) incubation of algal extract with metal precursor solution (Sharma et al., 2016). The reaction is initiated by mixing the liquid algal extract with the molar solution of metal precursor. Typically, the colour change of the reaction mixture demarcates as a visible signature for the initiation of reaction illustrating nucleation, followed by growth of NPs in which the adjoining nucleonic particles club together, thus forming thermodynamically stable NPs of different size and shape (Sharma et al., 2016; Prasad et al., 2016; Fawcett et al., 2017). The bioactive component of extract supports the

cascade of nanoparticle synthesis and the controlling factors involved are pH, temperature, concentration and time. Keeping aside the controlling factors, there are two routes of synthesis i.e. extracellular and intracellular. Initially, the nanoparticle synthesis was reported to be intracellular (Lengke et al., 2007a) but later algae were exploited for an extracellular mode of synthesis (Dahoumane et al., 2012b; Aboelfetoh et al., 2017; Fawcett et al., 2017).

4.1. Intracellular mode of synthesis of nanoparticles

The term "intracellular" refers to the process which takes place inside the cell. There is no requirement for any pre-treatment of microalgae because the process relies on metabolic pathways likely to be responsible for synthesis such as photosynthesis, respiration and nitrogen fixation (Sharma et al., 2016). The reducing agents may be NADPH or NADPH dependent reductase in the energy generating steps during photosynthesis *via* electron transport system (ETS) or may be respiratory ETS at thylakoid membranes (Sicard et al., 2010) or at the cell wall (Senapati et al., 2012).

An example is of *Rhizoclonium fontinale* and *Ulva intestinalis* when treated with chloroauric acid for 72 h at 20 °C; there was a visual change in the colour of thallus from green to purple confirming the fabrication of Au-NPs. This was supported by the fact when the gold solution was incubated with dried biomass there was no change in colour, which affirms that the bioreduction process is not associated with any of the metabolic pathways involving enzymes or other metabolites and the cells were poisoned by Au^{3+} when converted to Au^0 (Parial et al., 2012a). Sicard et al. (2010) encapsulated *Klebsormidium flaccidum* in silica gel suspension. The evident colour change of chloroplasts from green to purple inside the cells demonstrated the capacity of the entrapped cells to reduce gold salts. TEM images showed dark spots of reduced gold salts in the thylakoid membranes suggesting involvement of enzymes (NADPH and NADPH dependent reductase) in the synthesis of nanoparticles (Sicard et al., 2010).

In line with this trend, Senapati and co-workers (2012) demonstrated the intracellular synthesis by the algal cell wall in *Tetraselmis kochinensis*. UV-visible spectroscopy clearly proved that there was no extracellular synthesis. The NPs were more densely present near the cell wall rather than the cytoplasmic area, which is most likely due to the presence of bioactive moieties responsible for bioreduction. Further XRD of gold nano-alga biofilm confirms the synthesis of NPs at the cell wall (Senapati et al., 2012). Another chlorophycean alga *Spirogyra submaxima*, was also found to be efficient in bioconversion of Au^{3+} to Au^0. After exposure to gold solution, colour of the biomass turned pinkish purple and Au-NPs were extracted using sodium citrate solution as a capping agent. The intracellular synthesis of crystalline gold was further supported by Bragg reflections of purple coloured biomass (Roychoudhury and Pal, 2014).

4.2. Extracellular mode of synthesis of nanoparticles

The term "extracellular" refers to the process which takes place outside the cell mainly supported by the exudates of cell metabolism comprising of metabolites, ions, pigments, various proteins (enzymes) and non-protein entities such as DNA, RNA, microbial by-products (hormones, antioxidants) and lipids (Mata et al., 2009; Vijayan et al., 2014). The algal biomass is subjected to rudimentary pre-treatments such as washing and blending (Dahoumane et al., 2016).

Kalabegishvili et al. (2012) hypothesized that the active moieties on the surface of cells are not solely responsible for the synthesis rather optimum concentration of metal precursor and a number of cells is essential. Gold NPs were customized by varying the cell number and dose of Au (III) ions. The presence of gold peak at 530 nm affirmed the extracellular synthesis assisted by biomolecules/ proteins and enzymes on the cell surface of *Spirulina platensis*. In addition, gold uptake is time dependent which takes place in two phases i.e. rapid phase in which metal ions are taken up quickly on the cell surface because of the presence of active biomolecules (amino, carboxylic, phosphate, thiol), and the slow phase in which metal ions cross the cell membrane using transport mechanisms of the cell (Kalabegishvili and Kirkesali 2012).

In another study, Parial and Pal (2014) reported extracellular synthesis of Au-NPs from *Lyngbya majuscula* and *Spirulina subsalsa,* where the gradual development of colour was a time-dependent convenient visible signature indicating massive bioconversion of Au^{3+} to Au^0 leading to a steady synthesis of Au-NPs (Parial and Pal, 2014). Shakibaie et al. (2010) were hesitant to confirm the exact mechanism involved in the synthesis of Au-NPs *via Tetraselmis suecica*. The gold NPs fabricated were not enzyme dependent as the organism is a non-thermophile since the clear band at 530 nm appeared after 90 °C. The formation and stabilization of Au-NPs at these conditions might be due to the presence of reducing agents such as polyols and water-soluble heterocyclic compounds respectively (Shakibaie et al., 2010). The dried biomass of epilithic green alga, *Prasiola crispa* was exercised to tailor spherical Au-NPs (Sharma et al., 2014a). The FT-IR spectrum clearly illustrated the extracellular production of protein and organic moieties which might be responsible for preventing agglomeration and facilitating synthesis. The colour of the algal biomass remained intact after the completion of the process, thus ruling out the intracellular mode. The authors believed an extracellular pathway was responsible indicated by the purple colour and an absorption peak at 535 nm (Sharma et al., 2014a).

Mata et al. (2009) coupled the recovery and reduction of gold nanospheres by brown alga *Fucus vesiculosus* extracellularly at varying pH. A two-stage approach was followed in which the initial introduction of metal precursor had no effect on the colour, however, a reduction of gold and a colour change was observed in the second stage by a large decrease in the concentration of Au ions and pH. They found that gold uptake and bioreduction was at its highest level at neutral pH 7, because both the processes took place simultaneously. Further, FT-IR analysis revealed that the hydroxyl groups present in the algal polysaccharides are the possible reducing and capping agents (Mata et al., 2009). Macrolaga *Sargassum wightii* was reported to synthesize stable and uniform gold nanospheres with an average diameter of 11 nm extracellularly in a shorter duration. Interestingly there was absence of capping material around NPs which were at a uniform distance and were not in physical contact as observed in TEM images (Singaravelu et al., 2007).

Fluorescent Au-NPs were successfully fabricated using the dried biomass of an edible freshwater epilithic red alga *Lemanea fluviatilis* (L.) C.Ag (Sharma et al., 2014b). The synthesis from an aqueous reaction mixture of chloroauric acid and *Lemanea fluviatilis* was found to be a function of reaction time as revealed by UV-visible spectra, which exhibited SPR at 530 nm. The NPs were stable up to 90 days as supported by the retention in red colour of the solution and negligible change in SPR band position. Proteins were believed to be the capping and reducing agents. The fabricated nanospheres were spherical and TEM images at low magnification corroborated that the NPs tend to assemble in chain-like structures (Sharma et al., 2014b; LewisOscar et al., 2016). Nitrate reductase helps in NADH dependent extracellular reduction of Au^{+3} to Au^0, and has been suggested to be involved in the synthesis of nanogold in freshwater alga *Chlorella pyrenoidosa* (Oza et al., 2012).

Apart from the intracellular and extracellular modes of synthesis of NPs, two research groups reported both the modes of synthesis simultaneously (Parial et al., 2012a, b; Jena et al., 2014). Though many theories and hypotheses have been postulated to date, not one could clearly explain the exact mechanism for the synthesis of NPs.

4.3. Factors controlling synthesis of nanoparticles

Physical factors such as pH, precursor concentration, reaction time, exposure time and temperature control the nucleation, formation and stabilization of NPs. These factors can be altered to change the size and

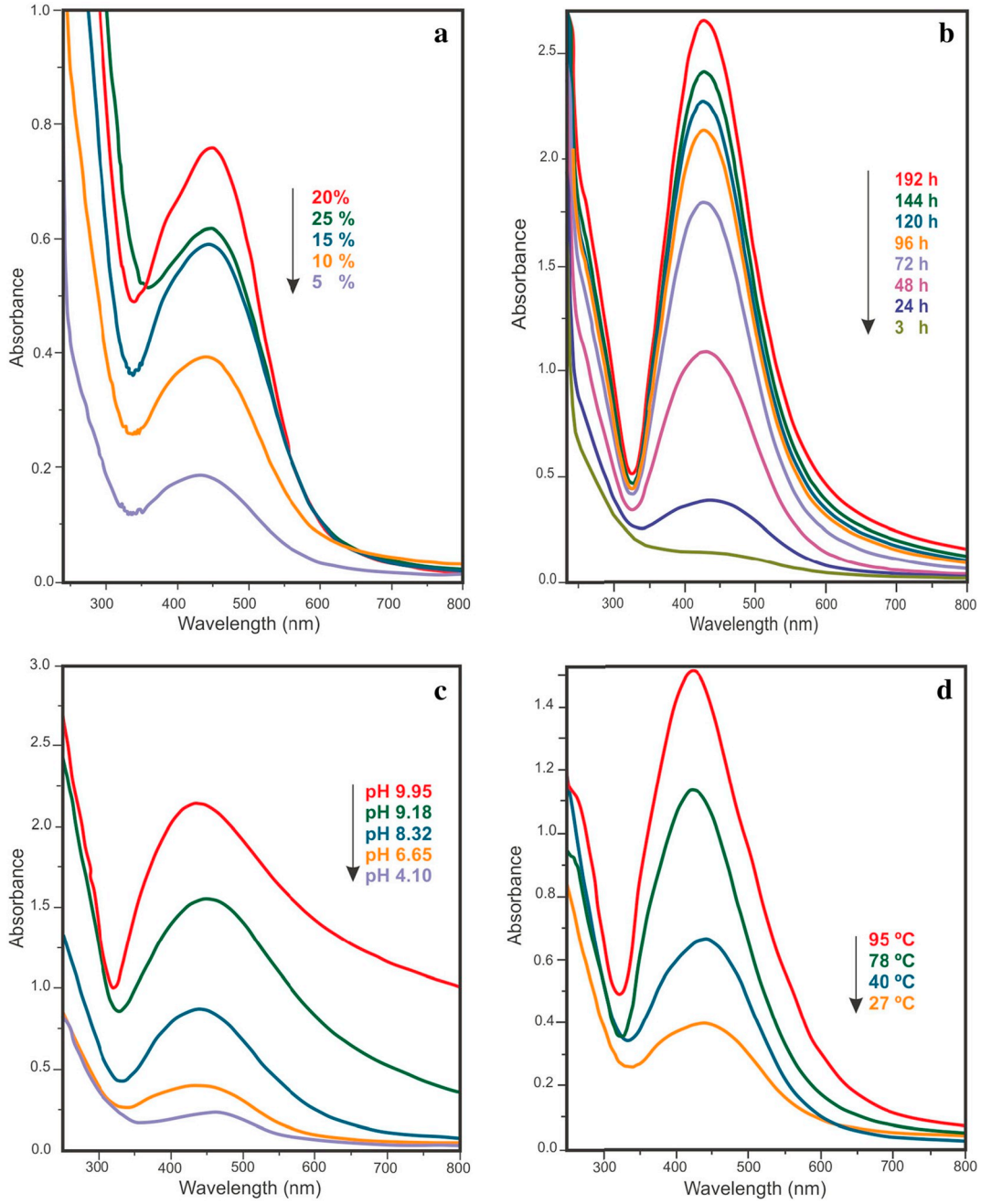

Fig. 5. UV–Vis spectra of Ag-NPs formed using 10^{-3}M $AgNO_3$ after 24 h at 27 °C with (a) various extract concentrations, (b) 10% extract as a function of contact time, (c) 10% extract at diverse pH values and (d) 10% extract at diverse temperatures (Abdel-Raouf et al., 2017).

morphology as well as to prevent agglomeration (Dahoumane et al., 2012b, 2014a, 2014b; Parial and Pal, 2015). The effect of extract concentration, pH, time and temperature were studied using UV-Vis spectroscopy (Fig. 5) for the optimization of synthesis of Ag-NPs using *Caulerpa serrulata* (Aboelfetoh et al., 2017).

4.3.1. Effect of extract concentration

Different concentrations of *C. serrulata* extract (5–25%) were added to 10^{-3} M $AgNO_3$ solution at room temperature after 24 h, and the effect was observed on Ag-NPs synthesis (Aboelfetoh et al., 2017). The increase in the concentration of extract from 5 to 20% lead to an increase in the SPR band intensity, causing a blue shift towards 435nm, indicating a decrease in average size of Ag-NPs (Fig. 5a). However, a further increase in the extract concentration up to 25% reduced the SPR band intensity which was perhaps due to particle agglomeration (Khalil et al., 2014; Velammal et al., 2016).

4.3.2. Effect of contact time

C. serrulata extract (10%) and Ag^+ ions were allowed to interact for 8 days at room temperature (Aboelfetoh et al., 2017). With gradual increase in contact time, SPR peak intensity increased without any shift leading to rapid synthesis of Ag-NPs. This clearly demonstrated the stability of Ag-NPs without agglomeration (Fig. 5b).

4.3.3. Effect of pH

Chromatic change in the reaction mixture and SPR band peak intensity were dependent on pH. The reducing and stabilizing power of *C. serrulata* extract was enhanced at basic pH. With an increase in pH from 6.65 to 9.95, a narrow SPR band at 427 nm was observed along with an increase in absorbance (Fig. 5c) (Aboelfetoh et al., 2017). However, in

acidic condition (pH-4.10), a broad SPR band was detected at 470 nm, reflecting the agglomeration of Ag-NPs or an increase in particle size, which indicates the formation of a large number of Ag-NPs with smaller diameter at higher pH values (Siddiqui et al., 2017).

4.3.4. Effect of temperature

Temperature plays a key role in the synthesis of Ag-NPs and at elevated temperature, the rate of reaction increases due to rapid utilization of reactants, leading to the formation of smaller NPs (Ibrahim, 2015). With increase in temperature from 27 to 95 °C, the less intense SPR band at 440 nm sharpens to 412 nm at 95 °C, decreasing the overall reaction time to 1 h (Fig. 5d) (Aboelfetoh et al., 2017).

5. Algae as a source for bionanomaterial

Algae are known to be one of the most primitive and influential biological entities existing autotrophically performing more than 50% of photosynthesis on this planet (Barsanti and Gualtieri, 2014). Being rich in biologically active compounds they are regarded as an appealing platform to serve as photosynthetic biorefineries capable of contriving a spectrum of high value-added products in addition to fuels (Jeffryes et al., 2015). Besides that, they are reported as hyperaccumulators of heavy metals and their chemical transformation and are believed to produce metal NPs (Zinicovscaia, 2012). Some of the pragmatic properties of the algae that make them as remarkable 'nanobiofactories' are (i) faster doubling time (Chisti, 2007) (ii) easily scalable and well developed systems (Chisti, 2007, 2008), (iii) cells can be readily disrupted (Chisti and Moo-Young, 1986), (iv) easily harvested (Grima et al., 2003) (v) low cost large-scale synthesis (Sharma et al., 2015b) and (vi) nucleation and crystal growth are accelerated due to the presence of negative charge on the surface of the cell (Sahoo et al., 2014). The chronicle, chemistry and the biological benefits of algae have been thoroughly discussed and documented elsewhere (Chen and Jiang, 2013; Namvar et al., 2015). More than a hundred different micro and macro algae have been reported that exhibit the ability to tailor NPs both intracellularly (Roychoudhury and Pal, 2014) and extracellularly (Mohseniazar et al., 2011), which can be recovered during downstream processing (Dahoumane et al., 2012a).

5.1. Gold nanoparticles

Conventionally, Au-NPs have been synthesized by physical and chemical processes (Table 1). These methods have been exploited extensively, however they have certain shortcomings such as release of unhealthy by-products, stringent chemicals, and are capital intensive (Shedbalkar et al., 2014). To refrain from the detrimental effects of toxic physicochemical techniques, research turned towards exploring living organisms. Enormous efforts have been made to understand the roles that organisms can play in the accumulation of gold and its conversion to non-toxic NPs (Parial et al., 2012a). The research in this niche has expanded rapidly with one or the other reports confirming the production of NPs by microbes (Baker et al., 2013). Rather than using all other biological entities, algae mediated synthesis is a straightforward approach for achieving the desired Au-NPs (Sharma et al., 2016).

Table 1
Physicochemical methods for synthesis of gold nanoparticle.

Synthesis of gold nanoparticles		
Physical method	**Chemical method**	**Physicochemical method**
● UV radiation ● Laser ablation ● Plasma synthesis	● Citrate synthesis ● Turkevich method ● Wet chemical synthesis ● Chemical reduction synthesis	● Sono-chemical ● Sono-electrochemical

However, the mechanism of synthesis, bioreduction, capping, and stabilization has been hypothesized by many researchers (Oza et al., 2012; Shabnam and Pardha-Saradhi, 2013; Parial and Pal, 2015; Namvar et al., 2015).

Algae have been proved as a boon with indefinite applications in numerous fields that have been employed as a substitute to chemical reductants for the tailoring of Au-NPs. Au-NPs have been synthesized from four different classes of algae such as *Cyanophyceae* (Blue-green algae) (Table 2), *Chlorophyceae* (Green algae) (Table 3), *Phaeophyceae* (Brown algae) (Table 4) and *Rhodophyceae* (Red algae) (Table 5). Material scientists have been consistently trying to fabricate Au-NPs by numerous methods with uniform size, shape, and monodispersity. It has been a challenging and vital mission to fabricate flexible and straightforward eco-friendly preparation methods to produce shape- and size-preferred Au-NPs (Namvar et al., 2015).

5.1.1. Synthesis of gold nanoparticles from cyanobacteria

Lengke et al. (2006a) used two different gold precursors [$AuCl_4^-$] and [Au $(S_2O_3)_2^{3-}$] and successfully demonstrated intracellular and extracellular synthesis of Au-NPs ranging in size from 10 to 25 nm. They used *Plectonema boryanum* UTEX 485 as a model organism because it is predominantly found in water bodies. In this study, cubical NPs and octahedral nanoplates were observed using TEM.

Parial et al. (2012a) performed a dual study of screening of potential algal strains and the effect of pH on the morphology of NPs. All three strains *Phormidium valderianum, Phormidium tenue* and *Microcoleus chthonoplastes* were able to synthesize NPs intracellularly. Among all *Phormidium valderianum,* could only synthesize gold nanospheres with a diameter of 15 nm at pH 5 along with triangular NPs (24 nm) at neutral pH and hexagonal NPs (25 nm) at basic pH 9. UV-Visible spectroscopy and TEM studies revealed the diversity in shapes and sizes of NPs. XRD peaks of the purple coloured biomass confirmed the reduction of Au (III) to Au (0) (Parial et al., 2012a).

Suganya et al. (2015) demonstrated the biosynthesis of Au-NPs using a protein extract of *Spirulina platensis* and 10 mM $HAuCl_4{\cdot}3H_2O$ in the ratio of 1:1. Addition of 1N NaOH under constant stirring for 3 h led to an instant colour change from green to greenish yellow. Further incubation of the reaction mixture at room temperature for 48 h produced a ruby red colour marking the formation of Au-NPs attributed to the collective oscillation of electron induction by the interacting electromagnetic field. Different UV-Vis peaks were observed at 685 nm, 524 nm and 385 nm for Au-NPs and *S. platensis* protein showed an excitation maximum at 620 nm. Stability of Au-NPs was evaluated at different temperatures (4, 15, 25, 60 and 80 °C) by monitoring λ_{max}. UV-Vis spectra revealed that Au-NPs were stable at 4-60 °C and at 80 °C stability was affected.

Many other researchers could collate the findings of the later by utilizing other species like *Plectonema boryanum* UTEX 485 (Lengke et al., 2006c), *Lyngbya majuscule* (Chakraborty et al., 2009), *Nostoc ellipsosporum* (Parial et al., 2012b) and *S. platensis* (Suganya et al., 2015) (Table 2). The factors affecting the morphology were mainly dependent on the cocktail of biological components present in the cell.

5.1.2. Synthesis of gold nanoparticles from green algae

The intracellular algae based synthesis of nano-gold was reported in unicellular green alga *Chlorella vulgaris* by Ting et al. (1995). Later on Xie et al. (2007a)) were successful in fabricating single-crystalline, triangular gold nanoplates from *Chlorella vulgaris.* They determined that there was a gold shaping protein (GSP of 28 kDa), involved in the bioreduction and shape regulation which was isolated and purified using SDS-PAGE and HPLC (Xie et al., 2007b).

Shakibaie et al. (2010) introduced the utilization of marine green microalgae *Tetraselmis suecica* for polydispersed and crystalline Au-NPs. The alternation of colour from yellow to red demonstrated the formation of spherical Au-NPs of size range 51-59 nm with an average size of 79 nm. They also tried to develop a rapid extracellular route, which was

Table 2
Cyanobacteria mediated synthesis of gold nanoparticles (Au-NPs).

Microalgae	Size & morphology	Application/Activity	Characterization	Bioreductant and capping agent	Reference
Plectonema boryanum UTEX 485	20–25 nm, cubic and octahedral gold plates	Synthesis of Au NPs from aqueous Au(I) thiosulfate and Au(III) chloride complexes in abiotic and cyanobacterial systems between 25-200 °C	TEM, SEM, XPS, TOF-SIMS	-	(Lengke et al., 2006a)
Lyngbya majuscula and *Spirulina subsalsa*	> 20 nm, spherical	Exposure to high concentration of Au salts can lead to synthesis initiation	TEM	Bioformation of Au NPs within the cells exposed in high gold level	(Chakraborty et al., 2009)
Synechocystis sp. PCC 6803	13 ± 2 nm, spherical	Intracellular biomineralization study	TEM, SERS, Zeta Potential	Carboxyl groups, polyphosphates, polysaccharides, cysteine or methionine compounds	(Focsan et al., 2011)
Nostoc ellipsosporum	20–40 nm, decahedral, icosahedra rods	Uniform distribution of aspect ratio of monodispersity	UV-Vis, TEM, DLS, Zeta Potential, XRD	Intracellular biotransformation, sodium citrate for extraction of nanorods	(Parial et al., 2012b)
Phormidium tenue	14.84 nm, spherical and irregular-shaped, fcc	Large-scale controlled synthesis of Au NPs	UV-Vis, TEM, XRD	Reduction of gold is associated with cellular metabolism and presumably involves reducing enzymes or synthesis of other metabolites	(Parial et al., 2012a)
Phormidium valderianum	pH 5: 15 nm, spherical, nanorods 411 × 32 nm pH 7: 7.92-17 nm, spherical; 24 nm triangular pH 9: 13.78 nm, spherical; 25 nm, hexagonal, fcc	Medicinally important gold nanorods	UV-Vis, TEM, XRD	Reduction of gold is associated with cellular metabolism and presumably involves reducing enzymes or synthesis of other metabolites	(Parial et al., 2012a)
Spirulina platensis	20–30 nm, spherical	Pharmaceutical technological purpose	UV-Vis, FT-IR, TEM, SEM-EDAX, XRD, NAA, AAS	Extracellular; biomolecules (amino, carboxylic, phosphate, thiol)	(Kalabegishvili et al., 2012)
Phormidium spp	25 nm, triangular	Antioxidant activity by DPPH, interaction with DNA, biolabelling	UV-Vis, HR-SEM, EDAX, FT-IR, TEM	Cytoplasmic protein moieties	(MubarakAli et al., 2013)
Lyngbya majuscule	2–25 nm, spherical, hexagonal	Low-cost production at ambient temperature and pressure	UV-Vis, TEM, DLS, XRD, FT-IR	Extracellular, Na citrate act as an capping agent, amino acid residue of protein shells act as stabilizer	(Parial and Pal, 2014)
Spirulina subsalsa	5–30 nm, spherical with few nanorods	Low-cost production at ambient temperature and pressure	UV-Vis, TEM, DLS, XRD, FT-IR	Extracellular, protein shells	(Parial and Pal, 2014)
Anabaena spp. (SAG 12.82)	10 nm, spherical	Self-reproducing bioreactor for *in vivo* biosynthesis	XRD, TEM	Protein or cellular enzymes	(Rösken et al., 2016)
Spirulina platensis	5 nm, spherical	Gram +ve strains: *B. subtilis* and *S. aureus;* stable for 2 months	UV-Vis, FT-IR, HR-TEM, EDAX	Carboxylate group in the reduction, Carboxyl, hydroxyl and primary amine are involved in stabilization	(Suganya et al., 2015)

Table 3
Green algae mediated synthesis of gold nanoparticles (Au-NPs).

Microalgae	Size & morphology	Application/Activity	Characterization	Bioreductant and capping agent	Reference
Green microalgae					
Chlorella vulgaris	0.8–2 μm along side, triangular, truncated triangular, hexagonal	Optical coatings and hyperthermia of cancer cells	TEM, FT-IR, AFM, XPS, HPLC, FESEM, SAED, UV-Vis	Gold shape-directing protein of 28kDa size	(Xie et al., 2007b)
Klebsormidium flaccidum	10–20 nm	Sol-gel methods for encapsulation of algal species within silica gels	UV-Vis, XRD, TEM, PAM, PEA, XPS, SERS	Insitu, gold reduction occurs in thylakoids where reducing enzymes	(Sicard et al., 2010)
Tetraselmis suecica	51–120 nm, spherical	First report on marine microalgae- based synthesis	UV-Vis, XRD, FT-IR	Extracellular, functional groups like -OH, -NH, -C=O of polyols and water-soluble heterocyclic compound	(Shakibaie et al., 2010)
Chlorella vulgaris	40–60 nm, spheroidal, polyhedral	Potentially attractive route to commercial production	XRD, TEM,XAS, AAS, XANES	Intracellular	(Luangpipat et al., 2011)
Klebsormidium flaccidum	9 ± 3.4 nm	Development of cell-based bioreactors for the production of metal NPs	PAM, TEM, UV-Vis	Intracellular	(Dahoumane et al., 2012)
Chlorella pyrenoidusa	25–30 nm, spherical, icosahedral, fcc	pH-dependent size controllable tuning of the synthesis of thermodynamically stable Au nanoparticle	UV-Vis, XRD, HR-TEM	NADH-dependent enzyme	(Oza et al., 2012)
Tetraselmis kochinensis	5–35 nm, spherical, triangular, fcc	Catalysis, electronics and coatings	UV-Vis, XRD, TEM	Intracellular, reduction by enzymes present in the cell wall and cytoplasmic membrane	(Senapati et al., 2012)
Coelastrella sp	30 nm sized spherical	Antioxidant activity by DPPH, interaction with DNA, biolabelling	UV-Vis, HR-SEM, EDAX, FT-IR, TEM	Cytoplasmic protein moieties	(MubarakAli et al., 2013)
Spirogyra submaxima	2–50 nm, spherical, triangular, hexagonal	Pure, easily extractable NPs are formed which can be used in biomedical applications	UV-Vis, DLS, XRD, TEM, Zeta Potential	Intracelluar synthesis at cell wall and the chloroplast	(Roychoudhury and Pal, 2014)
Cosmarium impressulum	5.7 ± 0.9 nm, spherical	Mechanism of synthesis studied thoroughly	UV-Vis, TEM	Enzymes and their cofactors	(Dahoumane et al., 2014b)
Green macroalgae					
Prasiola crispa	5–25 nm, fcc, spherical	Facile, one step and eco-friendly for the large scale synthesis	UV-Vis, XRD, FT-IR, DLS, HR-TEM	Protein and other molecules, extracellular	(Sharma et al., 2014a)
Rhizoclonium fontinale	pH 5: 5–20 nm spherical, 15–88 nm nanotriangles, 34 nm nanohexagons, rod-shaped (~100 × 51.5 nm); pH 7: spherical 13-22 nm, pH 9: 16 nm, nanospheres	Concentration of Au ions, pH and time play a vital role in synthesis. Alkaline pH induces formation of monodisperse nanoparticle	UV-Vis, HR-TEM, DLS, EDAX	Intracellular synthesis which is concentration dependent	(Parial and Pal, 2015)

Table 4
Brown algae mediated synthesis of gold nanoparticles (Au-NPs).

Macroalgae	Size & morphology	Application/Activity	Characterization	Bioreductant and capping agent	Reference
Sargassum sp.	300-400 nm along longest edge, 8-10 nm in thickness, fcc, hexagonal, truncated triangular,	Effect of pH, temperature, concentration, aging time, reaction time on the morphology of NPs	AFM, TEM, XRD, UV-Vis, FT-IR	Carbonyl, hydroxyl, amine functional groups and tannic materials	(Liu et al., 2005)
Sargassum wightii	8-12 nm, thin planer structure	Development of bioprocess for synthesis	UV-Vis, XRD, HR-TEM,	Biotransformation using algal species. Extracellular synthesis.	(Singaravelu et al., 2007)
Fucus vesiculosus	20–50 nm, spherical	Biogenic mechanisms of gold deposition involved in the formation of natural deposits	XRD, SEM, EDS, TEM, FT-IR, FAAS	Hydroxyl groups in polysaccharides of the algal cell wall, extracellular synthesis	(Mata et al., 2009)
Laminaria japonica	15–20 nm, spherical, crystalline, fcc	Extracellular biomineralization	UV-Vis, TEM, XRD, FT-IR,	Amide-I and amide-II groups of peptides and/or proteins	(Ghodake and Lee, 2011)
Turbinaria conoides	20–80 nm, crystalline	Mechanism of biosorption and bioreduction	UV-Vis, SEM, FE-SEM, EDX, XRD	Hydroxyl groups of polysaccharides	(Vijayaraghavan et al., 2011)
Sargassum myriocystum	15 nm; triangular and spherical, polydispersed	Cardiovascular treatment	UV-Vis, FT-IR, TEM, SEM-EDAX, XRD, GC-MS	1-cyclopentyl-4-(3 cyclopentylpropyl) dodecane	(Stalin Dhas et al., 2012)
Stoechospermum marginatum	18.7 to 93.7 nm, spherical, triangular and hexagonal	Antibacterial against Gram -ve *E. faecalis*	PL, SEM, TEM, XRD, FT-IR, WD-XRF	Hydroxyl groups present in the diterpenoids	(Rajathi et al., 2012)
Turbinaria conoides	6–10 nm, spherical	Antibacterial, biocompatible	UV-Vis, XRD, FT-IR, TEM	Fucoidan and polyphenolic groups	(Rajeshkumar et al., 2013a)
Turbinaria conoides	60 nm, triangle, rectangle and square	High antibacterial activity against *Streptococcus* sp, and medium for *B. subtilis* and *K. pneumoniae*	SEM, EDS	Biochemical material	(Rajeshkumar et al., 2013b)
Padina gymnospora	8–21 nm, spherical	Antitumor on liver cancer (HepG2) cell line	UV-Vis, XRD, AFM, HR-TEM, FT-IR	Fucoxanthin or flavonoids	(Singh et al., 2014a, 2014b)
Padina gymnospora	53–67 nm, fcc, nanoprisms and nano spheres	Cancer therapeutics	UV-Vis, FT-IR, AFM, SEM, XRD	Secondary metabolites, such as alkaloids having functional groups of hydroxyl, amines, alcohols, phenol and carboxylic acids	(Singh et al., 2013)
Dictyota bartayresiana	Spherical, poly-dispersed NPs	Antifungal against *Humiclo insulans* and *Fusarium dimerum*	UV-Vis, FT-IR, SEM	Carboxylic, amine and polyphenolic groups	(Varun et al., 2014)
Turbinaria conoides	2–19 nm, triangular, fcc	-	UV-Vis, FT-IR, XRD, FESEM, EDX, HR-TEM, CLSM	Free hydroxyl group and a carboxylic acid group	(Vijayan et al., 2014)
Ecklonia cava	20–50 nm, spherical, triangular, fcc	High antimicrobial activity against *E. coli* and *A. niger,* biocompatible as nontoxic for HaCaT cell lines	UV-Vis, XRD, FT-IR, FESEM-EDX, TEM	Biomolecules with primary amine group, hydroxyl group	(Venkatesan et al., 2014)
Sargassum muticum	5.42 ± 1.18 nm, spherical, fcc	Biomedical and pharmaceutical	UV-Vis, TEM, Zeta Potential, XRD	Capping of anionic bio-compounds, Bio-organic compounds/proteins	(Namvar et al., 2015)
Turbinaria conoides	12-57 nm, anistropic, poly-dispersed	Higher catalytic activity for reduction of aromatic nitro compounds and organic dye molecules	UV-Vis, HR-TEM, FT-IR, DLS, Zeta potential	Polyphenolic substances, hydroxyl group may act as capping agent	(Ramakrishna et al., 2016)
Sargassum tenerrimum	5–45 nm, anistropic, poly-dispersed	Dose dependent degradation of dyes like Rhodamine B, Sulforhodamine 101	UV-Vis, HR-TEM, FT-IR, DLS, Zeta potential	Secondary metabolites such as amino acids, alkaloids, carbohydrates, flavonoids, saponins, sterols, tannins, proteins and phenolic acids, hydroxyl group may act as capping agent	(Ramakrishna et al., 2016)
Cystoseira baccata	8.4 ± 2.2 nm, spherical, polycrystalline	Cytotoxic effect against human colon cancer cell lines HT-29 followed by Caco-2; biocompatibility with healthy cell line PCS-201-010	UV–Vis, TEM, HR-TEM, STEM, EELS, EDS, FT-IR, Zeta potential	Bioreduction by polyphenols and polysaccharides; Capping by proteins; Metal complexation by sulfonic groups from polysaccharides	(González-Ballesteros et al., 2017)

Table 5
Red algae mediated synthesis of gold nanoparticles (Au-NPs).

Macroalgae	Size & Morphology	Application/Activity	Characterization	Bioreductant and capping agent	Reference
Kappaphycus alvarezii	10–40 nm, polydisperse	Antibacterial against *Pseudomonas flouresences, S. aureus*	UV-Vis, XRD, TEM, FT-IR,FAAS	Extracellular, polyphenol compounds	(Rajasulochana et al., 2012)
Chondrus crispus	30–50 nm, spherical, polyhedral	Synthesis and possible route of metal recovery by sorption on the biomass surface	UV-Vis, TEM, SEM, EDS, FT-IR, FAAS	Stabilised in solution by amide I & II of proteins and xanthates	(Castro et al., 2013)
Galaxaura elongata	3.85–77.13 nm, rod, triangular, truncated, triangular, hexagonal	Antibacterial against *E. coli, K. pneumonia, S. aureus* and *Pseudomonas aeruginosa*	TEM, FT-IR, Zeta Potential, GC-MS, HPLC	Palmitic acid acts as stabilizing agent. Epigallocatechin catechin and epicatechin gallate are polyphenol compound as capping agents	(Abdel-Raouf et al., 2017)
Gracilaria corticata	45–57 nm	Gram +ve: *S. aureus, Enterococcus faecalis* Gram -ve: *E. coli, Enterobacter aerogenes* Antioxidant study by DPPH and ferric ion reducing ability	UV-Vis, SEM	Bioreduction	(Naveena and Prakash, 2013)
Lemanea fluviatilis (L.)	5–15 nm, nearly spherical polydispersed,	Antioxidant activity	UV-Vis, XRD, FT-IR, DLS, TEM, XRD	Protein and other organic molecules, extracellular	(Sharma et al., 2014b)

comparatively cheaper and convenient for downstream processing (Shakibaie et al., 2010).

Using dried biomass of a fresh water green alga, *Prasiola crispa* resulted in extracellular biosynthesis of highly stable nearly spherical Au-NPs. The progress of the reaction was routinely monitored by UV-Vis spectrum and colour change (yellow to purple). SPR band around 530 nm was observed after 1 h, which red shifted to 535 nm after 12 h, due to an increase in size with time. The differential intensity related to particle size distributions of Au-NPs was obtained from DLS study, which revealed average particle diameter and the cumulative mean diameter to be 10.0 ± 8.6 nm and 30.1 nm respectively. Greater particle size and high polydispersity observed in DLS in comparison to TEM are attributed to the fact that the measured size also included the biomaterials covering the surface of Au-NPs (Sharma et al., 2014a).

While searching for a suitable algal bioreagent for monodispersed Au-NPs, Parial and Pal (2015) reported a marine macroalgal strain *Rhizoclonium fontinale* which synthesized monodispersed gold nanospheres of 16 nm size with a maximum yield at pH 9. Variation in the physicochemical growth parameters like cell wall thickening, rapid akinete formation, pigment loss, giant cell formation, pyknosis, and purple coloration of the filaments during algae-gold interaction provided evidence for the synthesis of Au-NPs. In the context of obtaining better yield and monodispersed NPs, the effect of different concentrations of gold ions, biomass and pH of the reaction mixture were also studied. Maximum yield was obtained when alga was incubated for 72 h at pH 9 with 15 mg L^{-1} $AuCl_4^{-1}$. Polydispersed nanotriangles (15-88 nm), nanohexagons (34 nm) and nanorods (~100 × 51.5 nm) were formed at pH 5 and nanospheres at pH 7 (Parial and Pal, 2015).

Other strains in which *in-situ* synthesis of Au-NPs were reported are *Klebsormidium flaccidum* (Sicard et al., 2010; Dahoumane et al., 2012a), *Spirogyra submaxima* (Roychoudhury and Pal, 2014), and *Tetraselmis kochinensis* (Senapati et al., 2012). *Chlorella vulgaris* (Luangpipat et al., 2011), *Chlorella pyrenoidusa* (Oza et al., 2012), *Prasiola crispa* (Sharma et al., 2014a) produced gold nanospheres extracellularly with varied applications (Table 3).

5.1.3. Synthesis of gold nanoparticles from brown algae

After an exhaustive screening of a large number of marine brown algae, *Sargassum* spp. was reported as a promising candidate for the fabrication of gold nanoplates (Liu et al., 2005). Hexagonal, truncated triangular and triangular gold nanoplates were fabricated by the reduction of aqueous $AuCl_4^-$ ions from seaweed extract. Gold nanoplates of size 200-800 nm could be regulated by altering the initial concentration of the reactants. It was observed that the formation of gold nanoplates was dependent on various environmental factors such as the age of seaweed extract including reaction conditions such as pH, ionic concentration, temperature and time (Liu et al., 2005). Singaravelu et al. (2007) synthesized highly stable Au-NPs *via* the extracellular mode involving biotransformation of chloroauric acid. The bio-reduction process was highly efficient with nearly 95% of Au ions reduced to Au-NPs of size 8-12 nm within 12 h. A rapid bioprocess to scale up the yield of Au-NPs was developed (Singaravelu et al., 2007). Efficient recovery of Au-NPs was reported in *Fucus vesiculosus* and the process was nutrient independent, harmless and at a favourable neutral pH. This approach can replace the traditionally used hydrometallurgical method for gold recovery (Mata et al., 2009) (Table 4).

Novel brown alga *Ecklonia cava* was found to have potential reducing agents which help in the synthesis of Au-NPs. The appearance of ruby red colour after 1 min at 80 °C indicated the formation of Au-NPs with spherical and triangular morphologies with an average size of 30 ± 0.25 nm. UV-Vis spectra recorded at 532 nm attributed to the formation of Au-NPs. FT-IR spectra revealed that at 1628 cm^{-1} an N–H bend can be assigned to the 1° amine groups of the proteins. The intense medium absorbance at 1223 and 1031 cm^{-1} (C–N stretch) is the characteristic of the aliphatic amine groups. X-ray diffraction pattern showed high purity of biosynthesized Au-NPs which exhibited four

prominent Bragg reflections at around 38.39°, 44.54°, 64.89° and 77.72° which were indexed on the basis of face-centered cubic (fcc) of gold crystal planes corresponding to (111), (200), (220) and (311) respectively (Venkatesan et al., 2014).

González-Ballesteros et al. (2017) also demonstrated the biosynthesis of Au-NPs using aqueous extract of the brown alga *Cystoseira baccata* and $HAuCl_4$ solution (0.01 M) after 24 h with continuous stirring at room temperature. The reaction took place in few a minutes with progress of the reaction regularly monitored by UV-Vis spectroscopy. The end point was observed after 24 h as SPR peak intensity was stabilized at 532 nm. However, a slight dip in the pH (5.4 to 4.5) of the solution was noticed after the completion of the reaction. Au-NPs recovered were spherical in shape (mean diameter of 8.4 ± 2.2 nm), stable and polycrystalline in nature as demonstrated by TEM, HR-TEM, STEM and zeta potential measurements (González-Ballesteros et al., 2017).

5.1.4. Synthesis of gold nanoparticles from red algae

Presently there are very few reports which are industrially significant on red algae mediated synthesis of Au-NPs. Abdel-Raouf et al. (2017) found aqueous and ethanolic extracts of *Galaxaura elongata* separately could assist the synthesis of Au-NPs. The time reported for bioreduction of ethanolic and aqueous extracts was 2–5 min and 3 h, respectively. The change in colour of the solution was observed in both instances; however, there was a slight shift in λ_{max} from 535 nm (aqueous) to 536 nm (ethanol) which affirmed the synthesis of Au-NPs. While FT-IR determined that the carbonyl group of amino acids and peptides of proteins was responsible for capping, GC-MS and HPLC determined that the exact compound involved as stabilizing agent was palmitic acid and capping of Au-NPs was done by polyphenol compounds (epigallocatechin, catechin and epicatechin gallate) (Abdel-Raouf et al., 2017). An aqueous extract of *Lemanea fluviatilis*, an edible freshwater epilithic red alga, was used to biosynthesize Au-NPs. The initial yellow colour of chloroauric acid solution turned to red in 12 h. SPR band at 530 nm affirmed the synthesis and stability as colour was retained for 3 months. Polydispersed, crystalline, nearly spherical NPs of 5-15 nm were synthesized. HR-TEM revealed lattice fringes between the two adjacent planes to be 0.231 nm apart which corresponded to the interplanar separation of the (111) plane of face-centered cubic (fcc) Au-NPs. FT-IR revealed algal proteins were responsible for the reduction and stabilization of the Au-NPs (Sharma et al., 2014b). The majority of Au-NPs obtained from red algae are either rich in antioxidant activity (Sharma et al., 2014b) or have probable applications in therapeutics (Naveena and Prakash, 2013) (Table 5).

5.2. Silver nanoparticles

Silver is known to be a good conductor of heat and electricity, however, the high price limits its application in the electrical industry (Keat et al., 2015). For some time, the antimicrobial potential of silver has been explored in many medical fields, and has been successfully tested against 650 pathogenic microbes (Annamalai and Nallamuthu, 2016). Among the various noble metallic NPs known so far silver NPs (Ag-NPs) have gained the most attention, exhibiting the highest level of commercialization, accounting for 55.4% of the NMs based consumer products existing in the market (313 out of 565) (Agnihotri et al., 2014). Consequently, nanosilver is eventually becoming the nucleus of the nano-industry. Ag-NPs have been synthesised from different microalgae and macroalgae belonging to *Cyanophyceae* (Table 6), *Chlorophyceae* (Table 7), *Rhodophyceae* (Table 8) and *Phaeophyceae* (Table 9).

5.2.1. Synthesis of silver nanoparticles from cyanobacteria

Plectonema boryanum UTEX 485 was explored for the synthesis of Ag-NPs for the first time by Lengke et al. (2007a). Both intracellular and extracellular modes of synthesis were reported with considerable variation in the size of NPs from less than 10 nm and 1–200 nm

Table 6
Cyanobacteria mediated synthesis of silver nanoparticles (Ag-NPs).

Microalgae	Size & Morphology	Application/Activity	Characterization	Bioreductant and capping agent	Reference
Plectonema boryanum UTEX 485	Intracellularly (< 10 nm) and extracellularly (1–200 nm), octahedral	Temperature-dependent size control of NPs	TEM, XPS, TEM-EDS	Utilizing nitrate by reducing nitrate to nitrite and ammonium, which is fixed as glutamine before death	(Lengke et al., 2007a)
Oscillatoria willei NTDM01	10–25 nm, spherical		UV-Vis, SEM, EDS, FT-IR	Extracellular, reduced in the presence of nitrate reductase, and stabilized by the capping peptide tyrosine and tryptophan	(Ali et al., 2011)
Spirulina platensis	10–15 nm, fcc	Live algal mass can used for synthesis	UV-Vis, XRD, TEM	Cellular reductases	(Mahdieh et al., 2012)
Aphanothece spp., *Oscillitoria* spp., *Microcoleus* spp., *Aphanocapsa* spp., *Phormidium* spp., *Lynhbya* spp.	44-79 nm, spherical	Antimicrobial against Gram + ve: *S. aureus, E. faecalis* Gram -ve: *E. coli, E. aerogenes*	UV-Vis, SEM, EDX	Bioactive compounds	(Sudha et al., 2013)
Spirulina platensis	30–50 nm, spherical	Gram-ve: *E. coli, Proteus vulgaris, K. pneumoniae* Gram +ve: *S. aureus, S. epidermidis, B. cereus*	UV-Vis, SEM, TEM, and FT-IR	Monosubstituted amide of proteins	(Sharma et al., 2015b)
Cylindrospermum stagnale NCCU-104	38–88 nm, pentagonal	Extracellular cell free biosynthesis	UV-Vis, SEM	Proteins in the cell extract	(Husain et al., 2015)
Microchaete NCCU-342	60–80 nm, spherical, polydispersed	Degradation of azo dye methyl red.	UV-Vis, TEM, DLS, Zeta potential	Cellular metabolites	(Husain et al., 2019)

Table 7
Green Algae mediated synthesis of nanoparticles (Ag-NPs).

Microalgae	Size & Morphology	Application/Activity	Characterization	Bioreductant and capping agent	Reference
Microalgae					
Chlorella vulgaris	11.2 nm rods, 28.3 ± 3.1 nm triangular	Ag nanoplates was found to be a kinetically controlled process, depending on the ratio of carboxyl groups to Tyr per peptide molecule, as a result of the interactions between carboxyl groups with Ag ions, Ag reaction intermediates, and Ag surface	UV-Vis, FESEM, HR-TEM	Simple bifunctional tripeptide (DDY-OMe) with one Tyr residue as the reduction source and two carboxyl groups in the Asp residues as shape directors	(Xie et al., 2007a)
Nannochloropsis oculata, Chlorella vulgaris	15 nm, fcc	Cost effective, ecofriendly	AAS, XRD, TEM	Extracellular production, Protein	(Mohseniazar et al., 2011)
Chlamydomonas reinhardtii	Rounded/rectangular *in vitro* 5 ± 1 to 15 ± 2 nm *in vivo* 5 ± 1 to 35 ± 5 nm	Understanding the role of diverse cellular protein in the synthesis and capping	UV-Vis, ICP- MS, SEM, TEM, EDAX, MALDI-TOF, MS	Cellular proteins *viz* histone (H4), CA, FNR, SOD, SBPase, ATP synthase, RuBP carboxylase, and OEE.	(Barwal et al., 2011)
Chlorella sp.	34 nm, spherical, fcc	Scale up method	UV-Vis, XRD, FT-IR, SEM	Enzymes or Protein	(Elumalai et al., 2013)
Chlorococcum humicola	16 nm, spherical	Gram -ve: *E.coli*	UV-Vis, XRD, SEM, EDX, TEM, FT-IR	Intracellular and extracellular synthesis, protein molecules	(Jena et al., 2013)
Scenedesmus sp.	36 nm, spherical, fcc	Biological synthesis	UV-Vis, XRD, FT-IR, SEM	Enzymes or protein	(Elumalai et al., 2013)
Scenedesmus	15–20 nm, spherical,	Gram +ve: *S. mutans* Gram -ve: *E. coli*	AAS, UV-Vis, TEM, XRD, FT-IR, DLS, TGA	Intracellular, extracellular synthesis biomolecules, proteins and peptides	(Jena et al., 2014)
Euglena gracilis	15–60 nm, spherical, polydisperse	Comparison of *in vitro* and *in*B203 *vivo* both	UV-Vis, ICP-AES, HR-TEM, EDAX, FT-IR	Primary amines of proteins	(Li et al., 2015a)
Euglena intermedia	6–24 nm, spherical, polydisperse	Comparison of *in vitro* and *in vivo* both	UV-Vis, ICP-AES, HR-TEM, EDAX, FT-IR	Primary amines of proteins	(Li et al., 2015a)
Chlorella vulgaris	8–20 nm, fcc	Cost effective bioreactor for the conversion of ionic form of metals to NMs	UV-Vis, XRD, FT-IR, TEM, DLS, Zeta Potential, SEM-EDAX,	Extracellular, aromatic groups in the protein moiety	(Satapathy et al., 2015)
Chlorella vulgaris	50–70 nm	Synthesis of NPs using the algal biomass produced by waste water treatment	UV-Vis, SEM, FT-IR	Amines, phenols and alcohols, ethers and aromatic rings as reducing agents	(Karthikeyan et al., 2015)
Chlorella pyrenoidosa	5–20 nm with average 12 nm, fcc	Gram -ve: *K. pneumoniae, A. hydrophila, Acenetobacter* sp.; Gram +ve: *S. aureus;* Photocatalytic agent: Degradation of methylene blue	UV-Vis, XRD, SEM-EDS, TEM, XRD, FT-IR,	(NH)C=O group within the cage of cyclic peptides	(Aziz et al., 2015)
Euglena gracilis	47 nm	-	UV-Vis, DLS, Zeta Potential, ToF-SIMS, ICP-MS	-	(Li et al., 2015b)
Chlorella vulgaris	5–50 nm, fcc	Gram -ve: *E. coli, P. aeruginosa,* Fungus: *Candida albicans*	UV–vis, FT-IR, SEM, XRD, TEM, SAED	Protein moieties	(Annamalai and Nallamuthu, 2016)
Macroalgae					
Ulva reticulata	40–50 nm, spherical	-	UV-Vis, FT-IR,SEM, XRD	Carboxylic acids, benzene rings, fluoroalkanes	(Dhanalakshmi et al., 2012)
Enteromorpha compressa	40–50 nm, spherical	-	UV-Vis, FT-IR,SEM, XRD	Benzene rings and hydrogen bonded alcohols	(Dhanalakshmi et al., 2012)
Urospora sp	20–30 nm, fcc, spherical	Gram +ve: *S. aureus, B. subtilis;* Gram -ve: *E.coli, P. aeruginosa, K. pneumonia,*	UV-Vis, XRD, FT-IR, HR-TEM	Hydrogen bonded hydroxyl group, carbonyl and alcoholic group	(Suriya et al., 2012)
Ulva fasciata	28–41 nm, spherical	*Xanthomonas campestris* pv. *Malvacearum*	UV-Vis, FT-IR, XRD, SEM and EDX.	1-(Hydroxymethyl)–2, 5, 5, 8A-tetramethyl decahydro-2-napthalenol as reducing agent; Hexadecanoic acid as stabilizing agent	(Rajesh et al., 2012)
Ulva lactuca	20–56 nm, spherical	Anticancer: Hep2, MCF7 and HT29 cancer cell lines	UV-Vis, FT-IR, XRD, SEM, TEM, EDAX,	Release of protein molecules	(Devi and Bhimba, 2012)
Chaetomorpha linum	3–44 nm, 30 avg.	Non toxic method	UV-Vis, FT-IR, SEM	Peptides (secondary amines), flavonoids and terpenoids	(Kannan et al., 2013a)
Ulva lactuca	48.9 nm, spherical	Photocatalytic degradation of methyl orange dye	U-Vis, FT-IR, Zeta Potential, HRSEM, XRD,	phenolic compounds, amines and aromatic ring	(Kumar et al., 2013a)
Ulva faciata,	7–20 nm, spherical	Antimicrobial	UV-Vis, TEM, FT-IR, GLC	-C-O- groups of polyols of polysaccharides; -C-O-SO_4- of sulphated polysaccharides.	(El-Rafie et al., 2013)
Codium capitatum	3–44 nm, 30 avg.	First report on using seaweed from the widespread *Codium* genus, non toxic	UV-Vis, EDX, FT-IR,	Amine, peptide and sulphate groups	(Kannan et al., 2013b)

(*continued on next page*)

Table 7 (*continued*)

Microalgae	Size & Morphology	Application/Activity	Characterization	Bioreductant and capping agent	Reference
Enteromorpha flexuosa (wulfen) J.Agardh	15 + 1.5 nm, circular	Gram + ve: *B. subtilis, S. aureus, E. faecalis, S. epidermidis,* Gram -ve: *E.coli, K. pneumonia* Fungus: *C. albicans, S. cerevisiae*	UV-Vis, XRD, TEM, EDS	Amines, peptides and secondary metabolites	(Yousefzadi et al., 2014)
Ulva lactuca	20 nm, spherical	Gram + ve: *Bacillus* sp., Gram -ve: *Pseudomonas* sp., *E.coli*	UV-Vis, XRD, TEM, SEM, FT-IR	Aromatic compound or alkanes or amine	(Sangeetha and Saravanan, 2014)
Ulva lactuca	20–50 nm, spherical	Gram + ve: *Bacillus* sp., *S. aureus* Gram -ve: *E. coli, K. pneumonia, P. aeruginosa* Fungus: *C. albicans, A. niger, C. parapsilosis*	UV-Vis, TEM, XRD, SEM, EDAX, TGA	Release of extracellular protein molecules	(Bhimba and Kumari, 2014)
Caulerpa racemosa	5–25 nm, 10 nm, fcc	Gram + ve: *S. aureus* Gram -ve: *P. mirabilis*	UV-Vis, XRD, TEM, FT-IR	Cyclic peptides in stabilization and reduction	(Kathiraven et al., 2015)
Ulva flexousa	2–32 nm, circular, fcc	Method of synthesis at room temperature.	UV-Vis, XRD, FT-IR, TEM	Peptides are involved in reduction, cage of cyclic peptides in stabilization	(Rahimi et al., 2014)
Ulva lactuca	20–35 nm, cubical, fcc	Control of malarial plasmids. *P. falciparum.*	UV–vis, FT-IR, EDX, SEM, XRD	Organic components	(Murugan et al., 2015)
Pithophora oedogonia	25–44 nm, cubical and hexagonal-shaped	Gram -ve: *E. coli, P. aeruginosa, V. Cholera, Shigella flexneri* Gram + ve: *B. subtilis, S. aureus, Micrococcus luteus*	UV-Vis, EDS, SEM, DLS, FT-IR	Phytochemicals as reducing agents and protein as capping agents	(Sinha et al., 2015)
Spirogyra	40-80 nm, spherical	First report for using Ag_2SO_4 as a salt Gram + ve: *S. aureus* Gram -ve: *E. coli*	UV-Vis, FT-IR, TEM and NTA	Proteins	(Pinjarkar et al., 2016)
Spirogyra varians	17.6 nm, fcc structure, quasi-spheres	Gram + ve: *S. aureus, B. cereus, L. Monocytogenes* Gram -ve: *S. typhimurium, E. coli, P. aeruginosa, Klebsiella*	UV-Vis, XRD, FT-IR, SEM	Amino, carboxylic, hydroxyl and carbonyl groups, quinine	(Salari et al., 2016)
Caulerpa serrulata	10 ± 2 nm, spherical, fcc structure	Catalytic reduction of Congo red Antibacterial activity Gram + ve : *S. aureus* Gram –ve: *Salmonella typhi, E. coli, P. aeruginosa, Shigella*	UV-Vis, FT-IR, XRD, HR-TEM, ^1H and ^{13}C NMR	Caulerpenyne and/or its derivatives	(Aboelfetoh et al., 2017)

respectively. They observed a decline in nitrate concentration at 25 °C, which suggests the intracellular reduction of nitrate to ammonia. Ammonia is further converted to the amide group of glutamines, which shows that bioreduction of $AgNO_3$ to Ag-NPs is dependent on metabolic pathways of cyanobacteria. However, the release of organic moieties from dead cells attributed to extracellular bioreduction.

Tsibakhashvili et al. (2011) carried out extracellular synthesis *via Spirulina platensis* and studied the effect of short term and long term exposure of Ag ions along with its dependence on concentration. The shape and recovery of the NPs depend on both the factors *viz* on day 1, with the observation of scarcely dispersed 1 mM long $AgNO_3$ aggregates, and on day 5, NPs were distributed more uniformly on the surface of cells and were recovered completely (Tsibakhashvili et al., 2011). Cell free aqueous extract of *Microchaete* NCCU-342 was exposed to various cultural and physical conditions for optimizing synthesis of Ag-NPs. Optimal synthesis of Ag-NPs was obtained with biomass quantity of 80 μg/ml at pH 5.5 and 60 °C with UV light exposure (60 min) and 1 mM $AgNO_3$. Spherical, polydispersed NPs of size in the range of 60-80 nm were synthesized as revealed by TEM and DLS (Husain et al., 2019).

Screening of cyanobacterial species *Aphanothece, Oscillatoria, Microcoleus, Aphanocapsa, Phormidium, Lyngbya, Gloeocapsa,* and *Synechococcus,* isolated from mangroves was performed by Sudha et al. (2013) and *Microcoleus* spp could only fabricate spherical Ag-NPs with an average diameter of 55 nm. Cyanobacterial mediated synthesis of Ag-NPs at large scale was conducted by Sharma et al. (2015b) (Table 6).

5.2.2. Synthesis of silver nanoparticles from green algae

Over the past decade, researchers have proved the vitality of green microalgae in fabrication of Ag-NPs (Barwal et al., 2011; Jena et al., 2013; Annamalai and Nallamuthu, 2016). Xie et al. (2007b) used the extract of economically important unicellular green alga *Chlorella vulgaris,* for the synthesis of silver nanoplates. Synthesis of Ag nanoplates is a kinetically controlled process in which hydroxyl groups in tyrosine residues are the most active functional groups responsible for Ag^+ ion reduction and anisotropic growth and the shape control is regulated by carboxyl groups in Aspartic acid and/or Glutamic acid of the protein fraction in the extract (Xie et al., 2007a). Barwal et al. (2011) reported *in vitro* and *in vivo* biosynthesis of rounded and rectangular Ag-NPs from *Chlamydomonas reinhardtii*. *In vitro* synthesis was found to be slower, taking 13 days, and so-formed NPs possessed size in the range of 5 ± 1 to 15 ± 2 nm, while *in vivo* synthesis was a comparatively faster process which took 10 h, and the NPs produced were in the range of 5 ± 1 to 35 ± 5 nm. The formed NPs were in the peripheral cytoplasm and the basal body (end of the flagella). Such NPs were observed to be associated with oxidative reductive machinery and proteins involved in photosynthesis, stress response and ATP synthesis, i.e. ATP synthase, RUBP carboxylase, ferredoxin $NADP^+$ reductase, superoxide dismutase, sedoheptulose-1,7-bisphosphatase and oxygen evolving enhancer proteins. The involvement of these proteins was confirmed by the alteration in size and biosynthesis rate of NPs in protein-depleted fractions (Sharma et al., 2016).

Chlorophyte *Chlorococcum humicola* was exploited for intracellular and extracellular biosynthesis of Ag-NPs using fresh extracts (*in vitro*) and whole cells (*in vivo*) (Jena et al., 2013). After incubation of algal extract and whole cells with $AgNO_3$ (5 mM) solution for 48 h at 28 °C, spherical, crystalline Ag-NPs ranging from 2 to 16 nm with fcc geometry were obtained. The binding of proteins to the Ag-NPs through free amine groups, cysteine residue and electrostatic attraction of carboxylic groups in the cell wall was reported which probably stabilized the Ag-NPs as revealed by FT-IR (Jena et al., 2013; Sharma et al., 2016). *Chlorella* spp. was tailored for the synthesis of Ag-NPs both intracellularly and extracellularly for their application as antibacterial agents (Satapathy et al., 2015; Annamalai and Nallamuthu, 2016), in wastewater treatment (Karthikeyan et al., 2015; Aziz et al., 2015) and for large-scale synthesis (Elumalai et al., 2013) (Table 7). Li and co-

Table 8
Red Algae mediated synthesis of nanoparticles (Ag-NPs).

Macroalgae	Size & Morphology	Application/Activity	Characterization	Bioreductant and capping agent	Reference
Gelidiella acerosa	22 nm, spherical, fcc	Antifungal against *Humicola insolens, Fusarium dimerum, Mucor indicus, Trichoderma reesei*	UV-Vis, SEM, TEM, XRD, FT-IR,	Aromatic compound or alkanes or amines	(Vivek et al., 2011)
Gracilaria edulis	12.5–100 nm, spherical	Downstream processing	UV-Vis, SEM, TEM, XRD, FT-IR,	Proteins while terpenoids are implicated in stabilization extra cellular synthesis	(Murugesan et al., 2011)
Acanthophora spicifera	48 nm, spherical	Antimicrobial against biofilm forming bacteria *S. typhii* and *S. flexneri*	UV-Vis, FT-IR, TEM	Alcohols and phenols, carboxylic acids and its derivatives and chloroalkanes	(Kumar et al., 2012b)
Gelidiella sp.	40–50 nm, spherical	Anticancer against Hep 2 cell lines	UV-Vis, XRD, FT-IR, SEM, EDS,	Protein molecules	(Devi et al., 2012)
Gracilaria dura	6.0 ± 2 nm, sphere	Antibacterial against *B.pumilus,* food preservation and wound dressing	EDX, SAED, XRD, TGA, DSC, TEM	Polymer	(Shukla et al., 2012)
Kappa phycus sp	52–104 nm	-	UV-Vis, AFM, FT-IR,	-	(Baskar, 2013)
Kappaphycus alverazii	73 nm, fcc	-	UV-Vis, XRD, FT-IR, SEM, EDX,	Polysaccharides and -C-O groups of glycogen	(Ganesan et al., 2013)
Gracilaria corticata	18–46 nm	Antifungal activity against *C. albicans* and *C. glabrata*	UV-Vis, FT-IR, TEM, DLS, Zeta Potential	Phenolic compounds, amide I group and aromatic rings were responsible for stabilization	(Kumar et al., 2013b)
Pterocladia capillacae,	7 nm, spherical	Gram +ve: *S.aureus* Gram -ve: *E.coli*	UV-Vis, TEM, FT-IR, GLC	Reducing sugar, carbonyl groups and sulphated polysaccharides	(El-Rafie et al., 2013)
Jania rubins	12 nm, spherical	Gram +ve: *S.aureus* Gram -ve: *E.coli*	UV-Vis, TEM, FT-IR, GLC	Carbonyl group from amino acid residues and proteins	(El-Rafie et al., 2013)
Gracilaria edulis	55–99 nm, fcc, spherical,	Anticancerous against Human PC3 cell lines and non-toxic to normal Vero cell lines	UV-Vis, EDX, FT-IR, FESEM, XRD	Free and bound amide groups	(Priyadharshini et al., 2014)
Gracilaria birdiae	20.3 nm, spherical	Gram -ve: *E.coli*	UV-Vis, TEM, FT-IR, DLS, Zeta Potential,	Reduction of the silver ions is coupled to the oxidation of the hydroxyl and carbonyl group	(de Aragao et al., 2016)
Acanthophora specifera	33–81 nm, cubic	Gram +ve: *S. aureus, B. subtillis*; Gram -ve: *Salmonella sp., E. coli* Fngus: *C. albicans*	XRD, FT-IR	Monosaccharide, polysaccharide, uronic acids and secondary metabolites	(Ibraheem et al., 2016)
Amphiroa fragilissima	Crystalline	Gram +ve: *B. subtilis, S. aureus*; Gram -ve: *E. coli, K. pneumonia, P. aeruginosa*	UV-Vis, FT-IR, XRD and	Peptides	(Sajidha and Lakshmi, 2016

Table 9
Brown algae mediated synthesis of nanoparticles (Ag-NPs).

Macroalgae	Size & morphology	Application/Activity	Characterization	Bioreductant and capping agent	Reference
Sargassum wightii grevilli	8–27 nm, spherical,	Gram +ve :*S. aureus, B. rhizoids* Gram -ve: *E. coli, P. aeruginosa*	UV-Vis, FT-IR, XRD, HR-TEM	Extracellular, oxidation of alcoholic group to aldehyde, carboxylate ions	(Govindaraju et al., 2009)
Sargassum ilicifolium	33–40 nm, spherical	Gram +ve: *S. aureus* Gram -ve: *E. coli, K pneumoniae, S. typhii, Vibrio cholera;* Cytotoxic against *Artemia salina*	UV-Vis, SEM, TEM	Biologically active compounds	(Kumar et al., 2012a)
Sargassum plagiophyllum	20–50 nm, spherical	-	UV-Vis, FT-IR,SEM, XRD	Presence of primary amines, carboxylic acids, benzene rings, acetates in the phytochemicals	(Dhanalakshmi et al., 2012)
Sargassum polycystum	5–7 nm, spherical, fcc	Gram +ve: *S. aureus* Gram -ve: *E. coli, P. aeruginosa, K. pneumonia* Anticancer against MCF-7 breast cancer cell lines	UV-Vis, FT-IR, HR-TEM, XRD, GC-MS	Hexadecane, hexadecanoicacid, cis -9- octadecanol, 1-eicosanol, octadecanoic acid	(Thangaraju et al., 2012)
Padina pavonica	10-72 nm, spherical, polydisperse	Cotton pathogens: Fungus: *Fusarium oxysporum* Bacteria: *Xanthomonas campestris*	UV-Vis, FT-IR, XRD, SEM, TEM.	Extracellular, terpenoids	(Sahayaraj et al., 2012)
Padina tetrastromatica	14 nm, spherical	Gram +ve: *Bacillus* spp, *B. Subtilis* Gram -ve: *Klebsiella planticola, Pseudomonas* sp	UV-Vis, XRD, TEM, FT-IR	Broalkanes engage in recreation the foremost role in the NPs synthesis	(Rajeshkumar et al., 2012b)
Turbinaria conoides	96 nm, spherical	Gram +ve: *B. subtilis* Gram -ve: *K. planticola*	XRD, SEM, FT-IR, UV-Vis	Amines and polyphenols	(Rajeshkumar et al., 2012a)
Padina gymnospora	25-40 nm, spherical	Gram +ve: *B.cereus* Gram -ve: *E. coli*	UV-Vis, TEM	Aqueous extract of *Padina gymnospora*	(Shiny et al., 2013)
Colpmenia sinusa	20 nm, spherical	Gram +ve: *S.aureus* Gram -ve: *E.coli*	UV-Vis, TEM, FT-IR, GLC	-C-O- groups of polyols of polysaccharides; -C-O-SO_4- of sulphated polysaccharides.	(El-Rafie et al., 2013)
Cystophora moniliformis	75 nm, fcc	Temperature-dependent variation of the size of NPs	XRD, UV-Vis, SEM, DLS EDAX, Zeta Potential	Metabolites, phenolic compounds	(Prasad et al., 2013)
Sargassum cinereum	45 to 76 nm, triangular	Gram +ve: *S. aureus,* Gram -ve: *S. typhi, E. aerogenes, P. vulgaris*	UV-Vis, SEM		(Mohandass et al., 2013)
Sargassum longifolium	30 nm, cubical	Anticancer against Hep 2 cell line	UV-Vis, SEM, EDS, FT-IR,	Extracelluar, terpenoids with aldehyde, ketone, carboxylic acid groups, carbonyl group form amino acid residues that form the NP capping	(Devi et al., 2013)
Sargassum muticum	5–15 nm, spherical	Antifungal, antiviral, antiplatelet, antiangiogenesis	FT-IR, XRD, TEM, UV–Vis	Sulfate and hydroxyl moieties of polysaccharides	(Azizi et al., 2013)
Scaberia agardhii	40–50 nm, polydispersed	Soil microbial community	UV-Vis, SEM, EDAX	Proteins/ enzyme in cell wall	(Prasad and Elumalai, 2013)
Turbinaria conoides	2–17 nm, spherical, fcc	*E. coli*, followed by *Salmonella* sp., *S. liquefaciens*, *A. hydrophila* Cytotoxicity & anticrustacean: *Artemia salina*	UV-Vis, FT-IR, XRD, FESEM, EDX, and HR-TEM, CLSM	Free hydroxyl group and a carboxylic acid group	(Vijayan et al., 2014)
Sargassum longifolium	40–85 nm, spherical, fcc	Antifungal: *A. fumigatus, C. albicans, Fusarium* sp. *S.longifolium*	SEM, XRD. TEM. FT-IR, UV-Vis, EDX	Proteins for capping; carboxylic groups involved in stability	(Rajeshkumar et al., 2014)
Sargassum polycystum C. Agardh	-	Antibacterial: *E. coli, Streptococcus pyogenes, P. aeruginosa, S. flexneri, Morengilla morrgani;* Cytotoxic: Dalton's lymphoma ascites (DLA)	UV-Vis, FT-IR, XRD	Capped by proteins and metabolites such as phenolic acid, carboxylic acid and flavonoids	(Kanimozhi et al., 2015)
Sargassum vulgare	10 nm, spherical	Anticancer: Human myeloblastic leukemic cells HL60, cervical cancer cells HeLa	TEM, FACS, XRD, HR-TEM, FT-IR, EDX	Alginate moieties, secondary OH groups	(Govindaraju et al., 2015)
Turbinaria ornata	22 nm, spherical, polydisperse	Gram +ve: *B. litoralis, Bacillus* sp., *Micrococcus* sp., *Corynebacterium* sp., *S. aureus* Gram -ve: *Flavobacterium* sp., *Pseudomonas* sp., *Shigella* sp., *Aeromonas* sp., *V. cholerae, E. coli, Salmonella* sp., *E. aerogens, Klebsiella* sp., *Chromohalobacter* sp. *Artemia marina* and *Balanus Amphitrite*	UV-Vis, FE-SEM, EDS, XRD, FT-IR	Organic moieties as stabilizing agents	(Krishnan et al., 2015)
Sargassum muticum	43–79 nm, spherical, crystalline, fcc	Ovicidal and ovideterrent activity against *Aedes aegypti, Anopheles stephensi,* and *Culex quinquefasciatus* Gram +ve: *B. subtilis* Gram –ve: *S. typhi* and *K. pneumoniae*	UV–Vis, FT-IR, SEM, EDX, and XRD	Sulfate or hydroxyl groups	(Madhiyazhagan et al., 2015)

workers (2015b) for the first time reported *in vitro* and *in vivo* biosynthesis of Ag-NPs from *Euglena* spp. and found that the decreased concentrations of silver ions in the solutions, which were treated with *Euglena gracilis* and *Euglena intermedia* were almost equal. They also confirmed that concentration of chlorophyll plays a role in controlling the size and primary amines are the potential bioreductants (Li et al., 2015b).

In addition, other green algal species like *Nannochloropsis oculata* (Mohseniazar et al., 2011), *Chlorococcum humicola* (Jena et al., 2013), *Euglena gracilis* (Li et al., 2015a), *Scenedesmus* sp. (Jena et al., 2014) etc. have been reported to synthesize Ag-NPs with variable shapes and applications (Table 7). Other macroalgae have been investigated extensively for the synthesis of Ag-NPs are *Enteromorpha compressa* (Dhanalakshmi et al., 2012), *Urospora* sp. (Suriya et al., 2012), *Codium capitatum* (Kannan et al., 2013b), *Pithophora oedogonia* (Sinha et al., 2015) and *Spirogyra varians* (Salari et al., 2016) (Table 7).

During synthesis of Ag-NPs, chromatic changes in the reaction mixture act as a visual marker affirming the continuity of the process. Kannan et al., 2013b observed an obvious change of brown to yellow colour after 48 h during reduction of $AgNO_3$ by the extract of *Codium capitatum* and a time-dependent increase in brown colour intensity at 422 nm. Moreover during reduction of $AgNO_3$ by *Chaetomorpha linum* extract, the same colour change was observed within 30 minutes and with the increase in incubation time, the brown colour intensity decreased at 422 nm *viz* characteristic absorption peak of Ag-NPs (Kannan et al., 2013a). The role of amines and peptides in reduction and stabilization of NPs was the same in both the cases (Kannan et al., 2013a, 2013b).

Ulva lactuca, cheap seaweed readily available in the coastal areas of south India has been widely exploited as a facile method of synthesis by various scientific groups. The synthesized Ag-NPs have varied applications (Table 7). Kumar et al. (2013a) successfully fabricated spherical Ag-NPs with an average size of 48.59 nm at room temperature within 48 h of incubation, biometrically (Table 7).

5.2.3. Synthesis of silver nanoparticles from red algae

Coralline algae (red seaweeds) grow extensively in the marine environment, which are being used for commercial production of agar and its derivatives (Table 8). Unlike the conventional green synthesis approaches, a rapid and novel microwave-mediated protocol was devised by Priyadharshini et al. (2014) for the synthesis of Ag-NPs extracellularly from *Gracilaria edulis*. The presence of quinines in the aqueous extract was found to be responsible for the synthesis of nanospheres of 55-99 nm size which was confirmed by FT-IR and FE-SEM. Vivek et al. (2011) obtained spherical Ag-NPs of an average size of 22 nm using the aqueous extract of the red alga *Gelidiella acerosa*. Ag-NPs present in the filtrate were well distributed as non-aggregates and showed a broad λ_{max} peak at 408 nm. Aromatic compounds, alkanes or amines were attributed to be the capping ligand of the Ag-NPs (LewisOscar et al., 2016). The algal polysaccharides present in the decoction of *Gracilaria birdiae* played triple roles, i.e. complex formation with silver ions, control of reduction and stabilization of Ag-NPs. Effect of pH and polysaccharide concentration of (0.02, 0.03 and 0.05%, v/v) was done to optimize the process. The resulting NPs were effective against *Escherichia coli* (de Aragão et al., 2016) (Table 8).

5.2.4. Synthesis of silver nanoparticles from brown algae

Prasad et al. (2013) employed Australasian brown marine alga *Cystophora moniliformis* for the first time. Effect of temperature on the size and agglomeration showed that at temperatures lower than 65 °C, spherical Ag-NPs with size range 50-100 nm and higher temperatures up to 95 °C, NPs of size greater than 2 μm were formed. The NPs so formed were of crystalline nature with FCC geometry as suggested by XRD pattern (Prasad et al., 2013). Madhiyazhagan et al. (2015) reported the synthesis of crystalline spherical Ag-NPs with FCC geometery, ranging from 43 to79 nm in size using the aqueous extract of the seaweed *Sargassum muticum*. The synthesis of silver nanospheres was confirmed through visual assessment as the colour of the solution turned from yellowish light brown to dark brown after the addition of 1 mM $AgNO_3$ to 5% (w/v) algal extract at 95 °C. Initially no SPR peaks were observed however after 120 min of incubation, a characteristic SPR band of Ag-NPs at 420 nm was reported and the peak steadily increased over time indicating the saturation of the peak along with complete reduction of $AgNO_3$ (Madhiyazhagan et al., 2015) (Table 9).

5.3. Algae-mediated synthesis of other nanomaterials

As discussed in the previous sections, different types of algal species were reported to synthesize gold and silver NPs. Synthesis of various other NPs such as ZnO-NPs, TiO_2, CdS, Pt, Pd, Fe_3O_4 have also been reported (Table 10). Lengke et al. (2006b) for the first time developed an alternative method to abiotic chemical methods for the synthesis of platinum NPs and platinum (II) organics from *Plectonema boryanum UTEX 485*. They investigated synthesis at temperatures ranging from 25 to 180 °C, and the optimal temperature was found to be 29 °C. The resulting NPs were spherical, connected with bead-like organic moieties released from dead cyanobacterial cells. However, the size could not be systematically studied as the variation in temperature and time was huge. Crystallization and re-crystallization were affected by temperature, at lower temperature amorphous behaviour was observed contrary to the crystalline structure at higher temperature (180 °C) (Lengke et al., 2006b). *Phormidium* was found to be a suitable candidate for the extracellular synthesis of copper NPs. The reduction of cationic copper was believed to be done by a 25 kDa metal chelating protein moiety in aerobic conditions at neutral pH and room temperature. The role of proteins in the stabilization of NPs was confirmed by SDS- PAGE and FT-IR (Rahman et al., 2009). The aqueous cellular extract of diazotrophic cyanobacterial strain *Anabaena* L31 was exercised for the synthesis of ZnO-NPs conjugated with shinorine, water-soluble UV-B absorbent. A sharp decline in the surface charge of the conjugate from +30.25 mV to 3.75 mV resulted from the changes in the surface functionalities after conjugation formation (Singh et al., 2014a, 2014b, Pathak et al., 2019).

Aqueous extract from *Sargassum plagiophyllum* was reported successfully for the fabrication of AgCl-NPs (Dhas et al., 2014) (Table 10). Advanced characterization techniques like UV-Vis, FT-IR, FE-SEM, HR-TEM and XRD were employed to confirm the formation of AgCl-NPs which could be used as antimicrobial agents (Dhas et al., 2014). While screening a candidate for the synthesis of ZnO-NPs, *Sargassum myriocystum* was found to be suitable and process optimization was done for its synthesis (Azizi et al., 2014). To optimize parameters resulting in the synthesis of 36 nm sized ZnO-NPs extracellularly, pH, temperature, concentration of seaweed extract and metal concentration were studied. *Sargassum muticum* was also reported to biosynthesize hexagonal ZnO-NPs with an average size of 4 nm (Azizi et al., 2014). *Sargassum muticum* is so far the only algal species whose aqueous extract could manoeuvre cubic Fe_3O_4 NPs at room temperature. Apart from XRD, FT-IR, FE-SEM, ED-XRF and TEM, vibrating sample magnetometer (VSM) was studied to check the magnetic behaviour. FT-IR revealed sulphated polysaccharides were efficient stabilizers and bioreductants (Mahdavi et al., 2013).

A rapid and simple method for complete reduction of Pd (II) ions to Pd NPs by aqueous extract *Chlorella vulgaris* was demonstrated by Arsiya et al. (2017). Gradual colour change of the solution from yellow to dark brown indicated the formation of Pd-NPs. The reaction was completed in 10 min as the characteristic peak of Pd (II) ions at 410 and 420 nm disappeared. Furthermore, the formation of Pd-NPs was confirmed by SPR peak range at 370-440 nm. Polyol and amide groups of the extract were assumed to be responsible for the reduction and stabilization as strong and intense peaks were observed at 1051 cm^{-1} (Carbohydrate v(C-O-C) of polysaccharides, Nucleic Acid (and other phosphate-containing compounds), 1641 cm^{-1} (amide or C=C

Table 10
Algae mediated synthesis of other nanomaterials (NMs).

Microalgae	NP	Size	Application/Activitys	Characterization	Bioreductant and capping agent	Reference
Cyanobacteria						
Plectonema boryanum UTEX 485	Pt	30 nm–0.3 μm, spherical	First study as an alternative method to abiotic chemical methods	SEM,TEM, XPS	Polysaccharides have abundant uronic acid subunits, which, through their carboxyl groups	(Lengke et al., 2006b)
Plectonema boryanum UTEX 485	Pd	> 30 nm, spherical, fcc	First viable alternative method	SEM, TEM, XPS, XRD	Organic materials	(Lengke et al., 2007b)
Spirulina platensis	Ag/Au bimetallic	17–25 nm, fcc,	Single cell protein as nanobiofactories	UV-Vis, FT-IR, XRD, HR-TEM	Polypeptide/proteins	(Govindaraju et al., 2008)
Anabaena flos-aquae	β-FeOOH	-	-	XRD, HR-TEM, SEM-EDS	Intracellular	(Brayner et al., 2009)
Calothrix pulvinata	β-FeOOH	-	-	XRD, HR-TEM, SEM-EDS	Intracellular	(Brayner et al., 2009)
Phormidium cyanobacterium	CuO	10–40 nm, quasi-spheres, crystalline	Proteins induced under metal stress play a dual role of hydrolysis of precursor salt to CONPs and stabilizing agent, as particle solution is stable at room temperature for more than a week	UV-Vis, TEM, SEM,EDAX, XRD, FT-IR, SDS-PAGE	Extracellular, 25 kDa protein fraction as capping agent	(Rahman et al., 2009)
Phormidium tenue NTDM05	CdS	5.1 ± 0.2 nm, spherical	Biolabelling	FT-IR. EDAX, TEM, UV-Vis	C-phycoerythrin, thiol groups partial capping along with biological molecules	(MubarakAli et al., 2012)
Anabaena strain L31	ZnO	80 nm, hexagonal	Environmental-friendly sunscreen filters	UV-Vis, XRD, SEM, TEM, FT-IR, SAED, DLS	Phycobiliproteins	(Singh et al., 2014a, 2014b)
Brown						
Sargassum muticum	Fe_3O_4	18 ± 4 nm, cubic shape	High functional bioactivity	UV-Vis, EDXRF, XRD, FESEM, VSM,FT-IR, TEM	Sulphated polysaccharides in the reduction process and the stabilization, extracellular synthesis	(Mahdavi et al., 2013)
Sargassum myriocystum	ZnO	36 nm, spherical, triangle, radial, hexagonal, rod, rectangle size	Natural nanomedicine against microbial infection.	UV–visible, DLS, AFM, SEM, EDX, TEM, XRD, FT-IR	Fucoidan water soluble pigments	(Nagarajan and Arumugam, 2013)
Sargassum plagiophyllum	AgCl	18–42 nm, spherical	Antibacterial properties	UV-Vis, FT-IR, EDAX, HR-TEM, FESEM,XRD	Role of C=C in the reduction	(Dhas et al., 2014)
Bifurcaria bifurcata	CuO	5 to 45 nm, spherical	Antibacterial	UV-Vis, FT-IR, XRD, TEM	Water-soluble compounds such as diterpenoids	(Abboud et al., 2014)
Sargassum ilicifolium	Pd	60–80 nm, spherical		SEM, UV-Vis		(Prasad and Padmesh, 2014)
Sargassum bovinum	Pd	5–10 nm, monodispersed, octahedral	Catalytic performance by electrochemical reduction of hydrogen peroxide (H_2O_2)	UV–Vis, TEM, XRD, EDX, FT-IR	Sulphated polysaccharides	(Momeni and Nabipour, 2015)
Sargassum muticum	ZnO	3–57 nm, hexagonal wurtzite structures	One pot method for synthesis	UV-Vis, XRD, FESEM	Sulfate and hydroxyl moieties of polysaccharide	(Azizi et al., 2014)
Sargassum muticum	ZnO	3–57 nm, hexagonal wurtzite structures	Antiangiogenic and antiapoptotic effects on Human liver cancer cell line (HepG2).	UV-Vis, XRD, FESEM	Sulfate and hydroxyl moieties of polysaccharide	(Sanaeimehr et al., 2018)
Green						
Klebsormidium flaccidum	β-FeOOH	-	-	XRD, HR-TEM, SEM-EDS	Intracellular	(Brayner et al., 2009)
Chlorella vulgaris	Pd	7 nm, spherical	Photosynthetically driven metal transformation	TEM, SEM, ICP-OES, XPS	NADPH	(Eroglu et al., 2012)
Chlamydomonas reinhardtii	Ag/Au bimetallic	10–20 nm, spherical	Impact of metals salts on cell viability and characteristics of the NPs	UV-Vis, TEM	Extracellular matrix	(Dahoumane et al., 2014a, 2014b)
Chlorococcum sp. MM11	Fe	20–50 nm, spherical	Remediation of toxic Cr(VI)	UV-Vis, TEM, DLS, FT-IR, EDAX	Carbonyl and amine bonds from polysaccharides and glycoproteins present in the algal cell wall	(Subramaniyam et al., 2015)

(*continued on next page*)

Table 10 (*continued*)

Microalgae	NP	Size	Application/Activitys	Characterization	Bioreductant and capping agent	Reference
Scenedesmus-24	CdS	120–175 nm, oval shape	Environmental remediation-based application	FT-IR, XRD, TEM	Hydroxly group, N-H bond of amino group	(Jena et al., 2015)
Chlorella vulgaris	Pd	5–20 nm, spherical, monodisperse, crystalline	Easy and fast bioprocess	UV-Vis, FT-IR, XRD, TEM	Polyol and amide groups	(Arsiya et al., 2017)
Red						
Gracilaria edulis	ZnO	66–95 nm, rod shaped	Anticancerous against PC3 cell lines	UV-Vis, EDX, FT-IR, FESEM, XRD	Quinines	(Priyadharshini et al., 2014)
Gracilaria	Ag/Au bimetallic	22–30 nm, spherical	Gram + ve *S. aureus* Gram –ve *K. pneumoniae*	UV-Vis, HR-SEM	-	(Ramakritinan et al., 2013)

stretching vibrations of aromatic rings), 2922 (C − H stretching of polyols) and 3417 cm^{-1} (O − H group of polyols) in the FT-IR spectrum (Arsiya et al., 2017).

5.4. Algae-mediated synthesis of bimetallic nanoparticles

Bimetallic NPs are composed of two different metals which combine in different ratios to show novel properties derived from the constituting metals. These NMs have drawn more interest than monometallic NMs due to the presence of an extra degree of freedom. Extracellular interaction of single-cell proteins of *Spirulina platensis* with aqueous $AgNO_3$ and $HAuCl_4$ was examined for the biosynthesis of Ag-NPs, Au- NPs and Ag-Au core shell NPs. The interaction of cyanobacterial biomass and the metal precursor solutions ($AgNO_3$ and $HAuCl_4$ each at 10^{-3} M) solely or in combination for 120 h at 37 °C led to significant chromatic changes due to the excitation of surface plasmon vibrations in the metal NPs. The visual change in the colour of the reaction mixture to yellowish brown (Ag-NPs), ruby red (Au-NPs) and purple to brown (Ag-Au bimetallic) was noticed. SPR λ_{max} bands were observed at 424, 530 for Ag-NPs, Au-NPs. However, for bimetallic NPs absorption peaks were observed at 509, 486 and 464 nm for 75:25, 50:50 and 25:75 (Au:Ag) mol concentrations, respectively. The gradual shift from 530 to 424 nm was commensurate with the increased mole fraction of silver. The size of the NPs observed for Ag-NPs was 7-16 nm, Au-NPs was 6-10 nm and for bimetallic Au-Ag NPs it was 17-25 nm (Govindaraju et al., 2008; Pathak et al., 2019).

Similarly, green alga *Chlamydomonas reinhardtii* has also been reported to synthesize bimetallic Ag-Au NPs intracellularly. Aqueous mixtures of $AgNO_3$ and $HAuCl_4{\cdot}H_2O$ in different ratios (Ag:Au::1:0, 3:1, 1:1, 1:3, 0:1, 0:2) was introduced to the culture broth at room temperature (22 °C) under controlled light and dark exposure of 8 h dark/16 h day light. The creation of NPs starts within the cell soon after the introduction of metal salts. It occurs in three stages, initially the noble metals get internalized and reduced to NPs. Then the NPs get entrapped in the extracellular matrix to achieve colloidal stability and later the NPs are released into the culture medium from the extracellular matrix. The NPs recovered had a round shape with a narrow size distribution. SPR bands were reported ranging between 420 nm (Ag) and 555 nm (Au) in a linear proportion to the stoichiometric ratio at which these two metals were added to the culture (Dahoumane et al., 2014a).

Ramakritinan et al. (2013) employed *Gracilaria* spp. to form Ag-NPs, Au-NPs and even bimetallic Ag-Au nanoalloys. The reduction of metal solutions to corresponding NPs and bimetallic nanoalloys was validated by a change in colour *i.e* for Ag-NPs (transparent to dark brown), Au-NPs (ruby red) and Ag-Au bimetallic NPs (pale pink). The corresponding λ_{max} peaks at 419 nm for Ag, 536 nm for Au, 504 nm for Ag/Au (1,1), 526 nm for Ag/Au (1,3) and 501 nm for Ag/Au (3,1) corroborated their synthesis. However, it was confirmed by SEM analysis that all the NPs formed were colloidal in nature.

6. Applications of metallic nanoparticles

Metallic NPs fabricated from various algal sources used a multidisciplinary approach resulting from the investigational use of NPs in biological systems (Iravani et al., 2014). They can compete with the conventional medicines and have been reported to have antibacterial (Sharma et al., 2015a), anticancerous (Govindaraju et al., 2015) and antifungal activities (Azizi et al., 2013). Apart from medicinal applications, the metal NPs have extensive applicability in electronics, optics, cosmetics, coatings (Singh et al., 2014a, 2014b), food packaging, sensing devices, space industries, therapeutics, bioremediation (Iravani et al., 2014), environmental health (Husain et al., 2019), mechanics, light emitters, nonlinear optical devices, chemical industries (Khan et al., 2017), and photo-electrochemical applications (Mukherji et al., 2012; Makarov et al., 2014) (Tables 2-10).

6.1. Antimicrobial activity

NPs have drawn increasing interest from every branch of medicine for their ability to deliver drugs in the optimum dosage range often resulting in increased therapeutic efficiency of the drugs, weakened side effects and improved patient compliance (Khan et al., 2017). Au-NPs fabricated from diverse seaweeds have multifaceted roles in the medical industry as antibacterial agents against both Gram +ve (Rajathi et al., 2012; Venkatesan et al., 2014) and Gram -ve bacterial pathogens (Rajeshkumar et al., 2013b; Venkatesan et al., 2014), as antifungal against *Fusarium dimerum* and *Humiclo insulans* (Varun et al., 2014) and antitumor activity against lung and liver cells *in vitro via* activation of cell death (Singh et al., 2014a, 2014b). The small size of NPs disrupts the membrane functions of cells (permeability or respiration) by adhering to its surface and consequently penetrating the cell and further, damaging the DNA (Vijayan et al., 2016).

Au-NPs synthesized from *Spirulina platensis* exhibited strong antibacterial activity against Gram +ve bacteria *(Bacillus subtilis* and *Staphylococcus aureus)* where vancomycin was taken as a positive control. Protein functionalized Au-NPs managed to penetrate through the thick peptidoglycan layer and damaged the cell (Suganya et al., 2015). The use of brown alga *(Turbinaria conoides)* has been reported for the synthesis of Au-NPs exhibiting maximum antibacterial activity against *Streptococcus* spp. The opportune bacteria *B. subtilis* has a minimum range and pneumonia fever causing bacteria *Klebsiella pneumoniae* has a medium range of inhibition (Rajeshkumar et al., 2013b). Au-NPs synthesized using *Stoechospermum marginatum* were evaluated for their antibacterial effects against *Enterobacter faecalis* and it was higher than that of the positive control tetracycline, and the minimum zone of inhibition was recorded against *K. pneumonia*. However, no inhibition was found against *Escherichia coli* (Rajathi et al., 2012). On the basis of the nature of the extract derived from *Galaxaura elongate* (powder, ethanol and ethanol free extract), different types of Au-NPs were synthesized. The corresponding Au-NPs fabricated were evaluated for their antibacterial activities. Maximum inhibition was observed for Au-NPs from ethanolic extract against *E. coli*, *K. pneumoniae* and MRSA (Methicillin-resistant *Staphylococcus aureus*) followed by Au-NPs from free ethanolic extract which only exhibited high activity against MRSA. However, Au-NPs from powder of *G. elongata* were found to be effective against *E. coli* and *K. pneumonia* (Abdel-Raouf et al., 2017). Extracellularly synthesized Ag-NPs from brown marine weed, *Sargassum wightii* were tested for bacteria isolated from silkworm *Bombyx mori* L. Excellent zone of inhibition was observed in all the test species of bacteria (*S. aureus, Bacillus rhizoids*, *E. coli* and *Pseudomonas aeruginosa)* (Govindaraju et al., 2009).

Ethanolic extract of *Acanthophora specifera* acted as both capping and reducing agent in tailoring the cubic shaped Ag-NPs of 33-81 nm effective against a wide range of microbes including Gram +ve (*S. aureus* and *B. subtillis)*, Gram -ve (*Salmonella* sp. and *E. coli*) and yeast strain *Candida albicans* suggesting it may be a proficient antimicrobial agent (Ibraheem et al., 2016). The synthesized Ag-NPs from cellular metabolites of *Microcoleus* sp acted as a strong antibacterial agent against *E.coli, Proteus vulgaris, Salmonella typhi, Vibrio cholerae, B. subtilis, S. aureus, Streptococcus* and *Corynebacterium* (Sudha et al., 2013). Fucoidan, water-soluble pigments in aqueous cell extracts were identified to be responsible for capping and reduction. The resulting ZnO-NPs were highly stable up to 6 months and were effective antibacterial agents against Gram +ve and Gram -ve bacteria (Nagarajan and Arumugam, 2013). Biocompatible Ag-NPs, biosynthesized from *Gracilaria corticata* have an effective antifungal activity against ubiquitous fungi and are opportunistic pathogens of immunocompromised hosts i.e. *Candida albicans* and *Candida glabrata*. Spherical, stable Ag-NPs of 18-46 nm range were obtained at 60 °C within 20 min (Kumar et al., 2013b). Synthesis of Ag-NPs using the aqueous extract of red seaweed *Gelidiella acerosa* as the reducing agent exhibited antifungal property against *Humicola insolens* (MTCC 4520), *Fusarium dimerum* (MTCC 6583), *Mucor indicus* (MTCC 3318), and *Trichoderma reesei* (MTCC 3929) (Vivek et al., 2011; LewisOscar et al., 2016). In another report, the effect of the algal (*Sargassum longifolium*) mediated Ag-NPs against the pathogenic fungi *Aspergillus fumigatus*, *C. albicans*, and *Fusarium* sp. was determined (Rajeshkumar et al., 2014; LewisOscar et al., 2016).

6.2. Antifouling agents

Several studies have revealed that "nano-functionalized materials" inhibit bacterial adhesion and biofilm formation on surfaces by coating techniques (Beyth et al., 2008, Roe et al., 2008) and impregnation or embedding NMs (Lellouche et al., 2009). Targeting novel receptors involved in biofilm formation is the best strategy to control problems caused by the biofilm in marine environments (Vijayan et al., 2016). Vijayan et al. (2014) did a comparative study of biosynthesized Ag-NPs and Au-NPs from *Turbinaria conoides*. Ag-NPs were found to be efficient in controlling biofilm formation in *E. coli* followed by *Salmonella* sp., *Serratia liquefaciens,* and *Aeromonas hydrophila,* whereas Au-NPs were almost ineffective. Also, spherical (2-17 nm) Ag-NPs were lethal to brine shrimp *Artemia salina* with LC_{50} value of 88.914 μL mL^{-1}, which affirms it as a potent anti-microfouling agent (Vijayan et al., 2014). A similar study was performed by Kumar et al. (2012a) in synthesizing Ag-NPs from *Sargassum ilicifolium* with size range 33-40 nm and evaluated its cytotoxicity in *Artemia salina* (Kumar et al., 2012a) (Table 9). Krishnan et al. (2015) suggested that the 'coat' made of phytagel and apcomin zinc chrome paint glazed with Ag-NPs synthesized from *Turbinaria ornata* can prevent microflora and macroflora. The synthesized Ag-NPs restricted the growth of 15 biofilm isolates with maximum inhibition in *E. coli* (71.9%) and a minimum in *Micrococcus* sp. (40%) due to the secretion of extracellular polymeric substances (EPS) from Gram +ve bacteria. These silver based NPs can initiate a new quest of green antifouling compounds as the cytotoxic study revealed 100% mortality for *Balanu samphitrite* larvae and 56.6% for *Artemia marina* at 250 μg ml^{-1} and demonstrated lower toxicity to non-target species (Krishnan et al., 2015).

6.3. Bioremediation

It has been found that nanomaterials provide a wonderful platform for remediating pollution caused by various industrial effluents. In a study done by Ramakrishna et al. (2016), aqueous extracts of brown algae (*Turbinaria conoides* and *Sargassum tenerrimum*) were used as a reducing agent for Au-NPs synthesis. Biosynthesized Au-NPs showed efficient catalytic activity for the reduction of aromatic nitro compounds (4-nitrophenol and p-nitroaniline) and organic dye molecules (Rhodamine B and Sulforhodamine 101). *T. conoides* exhibited greater catalytic potential than *S. tenerrimum.* The Ag-NPs fabricated from *Ulva lactuca* actively degraded methyl orange photocatalytically under visible light illumination using silver as a nanocatalyst (Kumar et al., 2013a). Murugan et al. (2015) highlighted that *Ulva lactuca* mediated synthesis of stable Ag-NPs can be employed at low dosages to actively reduce populations of chloroquine-resistant *Plasmodium falciparum*. The smoke repellents based on *Ulva lactuca* may be cheaper and safer than the permethrin coils available in the market (Murugan et al., 2015). Ag-NPs synthesized from *Microchaete* NCCU-342 exhibited appreciable dye decolorization ability of azo dye methyl red as compared to cyanobacterial extract. Ag-NPs exhibited excellent photocatalytic activity against dye molecules and can be used in remediating pollution due to dyes and also in water purification systems (Husain et al., 2019). Intracellular synthesis of cadmium sulphide NPs was demonstrated in lipid-producing green alga *Scenedesmus*-24 (Table 10). The adsorption and adsorption kinetics of Cd (II) followed Langmuir isotherm pattern and Lagergren's pseudo-second-order model respectively, collectively signifying a chemisorbed monolayer of cadmium ions irreversibly bound on the algal biomass. The high retention of cadmium by the alga substantiates *Scenedesmus*-24 as a model microalga for bioremediation (Jena et al., 2015).

6.4. Other applications

The aqueous cellular extract of diazotrophic cyanobacterial strain *Anabaena* L31 was exercised for the synthesis of ZnO-NPs conjugated with shinorine, water-soluble UV-B absorbent. A sharp decline in the surface charge of the conjugate from +30.25 mV to 3.75 mV resulted from the changes in the surface functionalities after conjugate formation. The resulting conjugate reduced the ROS generation by up to 75%, which makes it a competent non-toxic sunscreen agent of biological origin (Singh et al., 2014a, 2014b). *Lemanea fluviatilis*, an edible freshwater epilithic red alga was used to biosynthesize Au-NPs, which showed remarkable antioxidant activity of the Au-NPs in the DPPH (2,2-diphenyl-1-picrylhydrazyl) assay (Sharma et al., 2014b). Catalytic performance of the biosynthetic Pd-NPs from *Sargassum bovinum* was investigated for electrochemical reduction of hydrogen peroxide (H_2O_2) (Momeni and Nabipour, 2015). Pd-NPs modified carbon ionic liquid electrode (Pd-NPs/CILE) was developed which gave a fast response time, high sensitivity and selectivity, and a low detection limit of H_2O_2, making it a promising electrochemical sensing platform.

7. Conclusion

Scientific breakthroughs have employed several algal systems for the synthesis of metal and metal oxide NPs. Low cultivation cost, less production time and eco-friendly synthesis minimize the use of hazardous chemicals that makes algae an alternative platform for the synthesis of NPs. Cyanobacterial strains such as *Spirulina* spp. and *Microcoleus* spp. have been explored to synthesize Ag-NPs with broad spectrum antibacterial activities against Gram +ve and Gram -ve bacteria. Au-NPs and Ag-NPs from members of Chlorophyceae such as *Chlorella* and *Ulva* show therapeutic potential against bacteria, fungi, protozoa and many cancerous cell lines. These are also being utilized in photocatalytic purification and remediation of polluted air and water, respectively. In addition, microalga *Scendesmus* is known for Cd retention and can be considered for the synthesis of Cd-NPs playing an important role in bioremediation. Among all algae, *Sargassum* spp. could be used to fabricate diverse kinds of NMs including Au-NPs, Ag-NPs, ZnO-NPs and TiO_2, opening a new scientific era for clinical diagnostics, therapeutic agents, fertilizers, biosensors, food packaging, cosmetics, paint, and biofilms. Different parameters (pH, temperature, concentration, and time), which decide shape and morphology of the NPs need to be optimized for specific products. Nevertheless, finite knowledge of synthesis mechanisms limits the use of a diverse range of algal species. Development of clean, bio-compatible, non-toxic and eco-friendly methods for the synthesis of the NPs is required (Gnanasangeetha and SaralaThambavani, 2013). Besides valuable implications, the issues related to environmental hazards generated due to heavy metals need to be considered to limit the serious affect NPs may have on the environment. Limitations ranging from variability of NP features due to the biological variability and different methodologies adopted to exploit these resources have impeded the path to quality control and market entrance. Emerging advanced characterization techniques would facilitate comparative and controlled performance of NPs, which will encourage judicious selection of algae-based NPs. Based on emerging reports presented in this review, in the future, a remarkable boom may be witnessed in the biosynthesis of algae-based NMs that will be likely to have enormous potential in pharmaceutics, agriculture, cosmetics and medicine.

Author contributions

PK and DG outlined the paper, and major contributions to the text for specific sections were written by PK. AK helped in data compilation. PK and DG contributed equally with general comments and editing the entire manuscript.

Declaration of Competing Interests

The authors have declared that no competing interests exist.

Acknowledgments

The authors are thankful to Director, Thapar Institute of Engineering and Technology, Patiala, Punjab, India.

References

Abboud, Y., Saffaj, T., Chagraoui, A., El Bouari, A., Brouzi, K., Tanane, O., Ihssane, B., 2014. Biosynthesis, characterization and antimicrobial activity of copper oxide nanoparticles (CONPs) produced using brown alga extract (*Bifurcaria bifurcata*). Appl. Nanosci. 4, 571–576.

Abdel-Raouf, N., Al-Enazi, N.M., Ibraheem, I.B., 2017. Green biosynthesis of gold nanoparticles using *Galaxaura elongata* and characterization of their antibacterial activity. Arab. J. Chem. 10, S3029–S3039.

Aboelfetoh, E.F., El-Shenody, R.A., Ghobara, M.M., 2017. Eco-friendly synthesis of silver nanoparticles using green algae (*Caulerpa serrulata*): reaction optimization, catalytic and antibacterial activities. Environ. Monit. Assess. 189 (7), 349.

Agnihotri, S., Mukherji, S., Mukherji, S., 2014. Size-controlled silver nanoparticles synthesized over the range 5–100 nm using the same protocol and their antibacterial efficacy. RSC Adv. 4, 3974–3983.

Ali, D.M., Sasikala, M., Gunasekaran, M., Thajuddin, N., 2011. Biosynthesis and characterization of silver nanoparticles using marine cyanobacterium, *Oscillatoria willei* NTDM01. Dig. J. Nanomater 6, 285–290.

Amendola, V., Meneghetti, M., 2009. Laser ablation synthesis in solution and size manipulation of noble metal nanoparticles. Phys. Chem. Chem. Phys. 11 (20), 3805–3821.

Annamalai, J., Nallamuthu, T., 2016. Green synthesis of silver nanoparticles: characterization and determination of antibacterial potency. Appl. Nanosci. 6, 259–265.

Anshup, Venkataraman J.S., Subramaniam, C., Kumar, R.R., Priya, S., Kumar, T.S., Omkumar, R.V., John, A., Pradeep, T., 2005. Growth of gold nanoparticles in human cells. Langmuir 21, 11562–11567.

Apolinário, A., Quitério, P., Sousa, C.T., Proença, M.P., Azevedo, J., Susano, M., Moraes, S., Lopes, P., Ventura, J., Araújo, J.P., 2014. Bottom-up nanofabrication using self-organized porous templates. J. Phys. Conf. Ser. 534, 012001.

de Aragao, A.P., de Oliveira, T.M., Quelemes, P.V., Perfeito, M.L.G., Araujo, M.C., Santiago, J.D.A.S., Cardoso, V.S., Quaresma, P., de Almeida, J.R.D.S., da Silva, D.A., 2016. Green synthesis of silver nanoparticles using the seaweed *Gracilaria birdiae* and their antibacterial activity. Arab. J. Chem. https://doi.org/10.1016/j.arabjc.2016.04.014.

Arbain, R., Othman, M., Palaniandy, S., 2011. Preparation of iron oxide nanoparticles by mechanical milling. Miner. Eng. 24 (1), 1–9.

Arsiya, F., Sayadi, M.H., Sobhani, S., 2017. Green synthesis of palladium nanoparticles using *Chlorella vulgaris*. Mater. Lett. 186, 113–115.

Asmathunisha, N., Kathiresan, K., 2013. A review on biosynthesis of nanoparticles by marine organisms. Colloids Surf. B: Biointerfaces 103, 283–287.

Aziz, N., Faraz, M., Pandey, R., Shakir, M., Fatma, T., Varma, A., Barman, I., Prasad, R., 2015. Facile algae-derived route to biogenic silver nanoparticles: synthesis, antibacterial, and photocatalytic properties. Langmuir 31, 11605–11612.

Azizi, S., Namvar, F., Mahdavi, M., Ahmad, M., Mohamad, R., 2013. Biosynthesis of silver nanoparticles using brown marine macroalga, *Sargassum Muticum* aqueous extract. Materials 6, 5942–5950.

Azizi, S., Ahmad, M.B., Namvar, F., Mohamad, R., 2014. Green biosynthesis and characterization of zinc oxide nanoparticles using brown marine macroalga *Sargassum muticum* aqueous extract. Mater. Lett. 116, 275–277.

Baker, S., Harini, B.P., Rakshith, D., Satish, S., 2013. Marine microbes: Invisible nanofactories. J. Pharm. Res. 6, 383–388.

Barsanti, L., Gualtieri, P., 2014. Algae: Anatomy, Biochemistry, and Biotechnology. CRC Press, Second Edition.

Barwal, I., Ranjan, P., Kateriya, S., Yadav, S.C., 2011. Cellular oxido-reductive proteins of *Chlamydomonas reinhardtii* control the biosynthesis of silver nanoparticles. J. Nanobiotechnol. 9, 56.

Baskar, B.B., 2013. Biosynthesis of silver nanoparticles using *Kappa phycus* species. Int. J. Res. Pharm. Sci. 3, 55–63.

Beyth, N., Houri-Haddad, Y., Baraness-Hadar, L., Yudovin-Farber, I., Domb, A.J., Weiss, E.I., 2008. Surface antimicrobial activity and biocompatibility of incorporated polyethylenimine nanoparticles. Biomaterials 29 (31), 4157–4163.

Bhaviripudi, S., Jia, X., Dresselhaus, M.S., Kong, J., 2010. Role of kinetic factors in chemical vapor deposition synthesis of uniform large area graphene using copper catalyst. Nano Lett. 10 (10), 4128–4133.

Bhimba, B.V., Kumari, P.R., 2014. Phytosynthesis of silver nanoparticles from the extracts of seaweed *Ulva lactuca* and its antimicrobial activity. Int. J. Pharm. Bio. Sci. 5, 666–677.

Brayner, R., Yéprémian, C., Djediat, C., Coradin, T., Herbst, F., Livage, J., Fiévet, F., Couté, A., 2009. Photosynthetic microorganism-mediated synthesis of akaganeite (beta-FeOOH) nanorods. Langmuir 25, 10062–10067.

Castro, L., Blázquez, M.L., Muñoz, J.A., González, F., Ballester, A., 2013. Biological synthesis of metallic nanoparticles using algae. IET Nanobiotechnol. 7, 109–116.

Chakraborty, N., Banerjee, A., Lahiri, S., Panda, A., Ghosh, A.N., Pal, R., 2009.

Biorecovery of gold using cyanobacteria and an eukaryotic alga with special reference to nanogold formation – a novel phenomenon. J. Appl. Phycol. 21, 145.
Chen, F., Jiang, Y. (Eds.), 2013. Algae and Their Biotechnological Potential. Springer Science & Business Media.
Cheng, W., Zhang, W., Hu, L., Ding, W., Wu, F., Li, J., 2016. Etching synthesis of iron oxide nanoparticles for adsorption of arsenic from water. RSC Adv. 6 (19), 15900–15910.
Chisti, Y., 2007. Biodiesel from microalgae. Biotechnol. Adv. 25, 294–306.
Chisti, Y., 2008. Biodiesel from microalgae beats bioethanol. Trends Biotechnol. 26, 126–131.
Chisti, Y., Moo-Young, M., 1986. Disruption of microbial cells for intracellular products. Enzym. Microb. Technol. 8, 194–204.
D'Amato, R., Falconieri, M., Gagliardi, S., Popovici, E., Serra, E., Terranova, G., Borsella, E., 2013. Synthesis of ceramic nanoparticles by laser pyrolysis: From research to applications. J. Anal. Appl. Pyrolysis 104, 461–469.
Dahoumane, S.A., Djediat, C., Yéprémian, C., Couté, A., Fiévet, F., Coradin, T., Brayner, R., 2012a. Recycling and adaptation of *Klebsormidium flaccidum* microalgae for the sustained production of gold nanoparticles. Biotechnol. Bioeng. 109, 284–288.
Dahoumane, S.A., Djediat, C., Yéprémian, C., Couté, A., Fiévet, F., Coradin, T., Brayner, R., 2012b. Species selection for the design of gold nanobioreactor by photosynthetic organisms. J. Nanopart. Res. 14, 883.
Dahoumane, S.A., Wijesekera, K., Filipe, C.D., Brennan, J.D., 2014a. Stoichiometrically controlled production of bimetallic Gold-Silver alloy colloids using micro-alga cultures. J. Colloid Interface Sci. 416, 67–72.
Dahoumane, S.A., Yéprémian, C., Djédiat, C., Couté, A., Fiévet, F., Coradin, T., Brayner, R., 2014b. A global approach of the mechanism involved in the biosynthesis of gold colloids using micro-algae. J. Nanopart. Res. 16, 2607.
Dahoumane, S.A., Wujcik, E.K., Jeffryes, C., 2016. Noble metal, oxide and chalcogenide-based nanomaterials from scalable phototrophic culture systems. Enzym. Microb. Technol. 95, 13–27.
Devi, J.S., Bhimba, B.V., 2012. Anticancer activity of silver nanoparticles synthesized by the seaweed *Ulva lactuca* invitro. Sci. Rep. 1, 242.
Devi, J.S., Bhimba, B.V., Ratnam, K., 2012. In vitro anticancer activity of silver nanoparticles synthesized using the extract of *Gelidiella* sp. Int J Pharm Pharm Sci 4, 710–715.
Devi, J.S., Bhimba, B.V., Peter, D.M., 2013. Production of biogenic silver nanoparticles using *Sargassum longifolium* and its applications. Indian J. Mar. Sci. 42, 125–130.
Dhanalakshmi, P.K., Azeez, R., Rekha, R., Poonkodi, S., Nallamuthu, T., 2012. Synthesis of silver nanoparticles using green and brown seaweeds. Phykos 42, 39–45.
Dhas, T.S., Kumar, V.G., Abraham, L.S., Karthick, V., Govindaraju, K., 2012. *Sargassum myriocystum* mediated biosynthesis of gold nanoparticles. Spectrochim. Acta A Mol. Biomol. Spectrosc. 99, 97–101.
Dhas, T.S., Kumar, V.G., Karthick, V., Angel, K.J., Govindaraju, K., 2014. Facile synthesis of silver chloride nanoparticles using marine alga and its antibacterial efficacy. Spectrochim. Acta A Mol. Biomol. Spectrosc. 120, 416–420.
El-Rafie, H.M., El-Rafie, M., Zahran, M.K., 2013. Green synthesis of silver nanoparticles using polysaccharides extracted from marine macro algae. Carbohydr. Polym. 96, 403–410.
El-Said, W.A., Cho, H.Y., Yea, C.H., Choi, J.W., 2014. Synthesis of metal nanoparticles inside living human cells based on the intracellular formation process. Adv. Mater. 26 (6), 910–918.
Elumalai, S., Santhose, B.I., Devika, R., Revathy, S., 2013. Collection, isolation, identification, and biosynthesis of silver nanoparticles using microalga *Chlorella pyrenoidosa*. Nanomech. Sci. Technol. Int. J. 4, 59–66.
Eroglu, E., Chen, X., Bradshaw, M., Agarwal, V., Zou, J., Stewart, S.G., Duan, X., Lamb, R.N., Smith, S.M., Raston, C.L., Iyer, K.S., 2012. Biogenic production of palladium nanocrystals using microalgae and their immobilization on chitosan nanofibers for catalytic applications. RSC Adv. 3, 1009–1012.
Fawcett, D., Verduin, J.J., Shah, M., Sharma, S.B., Poinern, G.E.J., 2017. A review of current research into the biogenic synthesis of metal and metal oxide nanoparticles via marine algae and seagrasses. J. Nanosci. 2017.
Focsan, M., Ardelean, I.I., Craciun, C., Astilean, S. 2011. Interplay between gold nanoparticle biosynthesis and metabolic activity of cyanobacterium *Synechocystis* sp. PCC 6803. Nanotechnology, 22(48), 485101.
Ganesan, V., Aruna Devi, J., Astalakshmi, A., Nima, P., Thangaraja, A., 2013. Eco-friendly synthesis of silver nanoparticles using a sea weed, *Kappaphycus Alvarezii* (Doty) Doty ex P.C.Silva. Int. J. Eng. Adv. Technol. 2, 559–563.
Ghodake, G., Lee, D.S., 2011. Biological synthesis of gold nanoparticles using the aqueous extract of the brown algae *Laminaria japonica*. J. Nanoelectron. Optoelectron. 6 (3), 268–271.
Ghorbani, H.R., 2014. A review of methods for synthesis of Al nanoparticles. Orient. J. Chem. 30 (4), 1941–1949.
Gnanasangeetha, D., SaralaThambavani, D., 2013. One pot synthesis of zinc oxide nanoparticles via chemical and green method. Res. J. Mater. Sci. 1, 1–8.
González-Ballesteros, N., Prado-López, S., Rodríguez-González, J.B., Lastra, M., Rodríguez-Argüelles, M.C., 2017. Green synthesis of gold nanoparticles using brown algae *Cystoseira baccata:* Its activity in colon cancer cells. Colloids Surf. B: Biointerfaces 153, 190–198.
Govindaraju, K., Basha, S.K., Kumar, V.G., Singaravelu, G., 2008. Silver, gold and bimetallic nanoparticles production using single-cell protein (*Spirulina platensis*) Geitler. J. Mater. Sci. 43 (15), 5115–5122.
Govindaraju, K., Kiruthiga, V., Kumar, V.G., Singaravelu, G., 2009. Extracellular synthesis of silver nanoparticles by a marine alga, *Sargassum wightii Grevilli* and their antibacterial effects. J. Nanosci. Nanotechnol. 9, 5497–5501.
Govindaraju, K., Krishnamoorthy, K., Alsagaby, S.A., Singaravelu, G., Premanathan, M., 2015. Green synthesis of silver nanoparticles for selective toxicity towards cancer cells. IET Nanobiotechnol. 9, 325–330.
Grima, E.M., Belarbi, E.H., Fernández, F.A., Medina, A.R., Chisti, Y., 2003. Recovery of microalgal biomass and metabolites: process options and economics. Biotechnol. Adv. 20, 491–515.
Gurentsov, E.V., Eremin, A.V., Schulz, C., 2007. Formation of carbon nanoparticles by the condensation of supersaturated atomic vapor obtained by the laser photolysis of C_3O_2. Kinet. Catal. 48, 194–203.
Guzmán, M.G., Dille, J., Godet, S., 2009. Synthesis of silver nanoparticles by chemical reduction method and their antibacterial activity. World Acad. Sci. Eng. Technol. 43, 357–364.
Hatakeyama, H., Akita, H., Harashima, H., 2011. A multifunctional envelope type nano device (MEND) for gene delivery to tumours based on the EPR effect: a strategy for overcoming the PEG dilemma. Adv. Drug Deliv. Rev. 63, 152–160.
Hulkoti, N.I., Taranath, T.C., 2014. Biosynthesis of nanoparticles using microbes—a review. Colloids Surf. B: Biointerfaces 121, 474–483.
Husain, S., Sardar, M., Fatma, T., 2015. Screening of cyanobacterial extracts for synthesis of silver nanoparticles. World J. Microbiol. Biotechnol. 31 (8), 1279–1283.
Husain, S., Afreen, S., Yasin, D., Afzal, B., Fatma, T., 2019. Cyanobacteria as a bioreactor for synthesis of silver nanoparticles-an effect of different reaction conditions on the size of nanoparticles and their dye decolorization ability. J. Microbiol. Methods 162, 77–82.
Ibraheem, I.B.M., Abd-Elaziz, B.E.E., Saad, W.F., Fathy, W.A., 2016. Green biosynthesis of silver nanoparticles using marine Red Algae *Acanthophora specifera* and its antimicrobial activity. J. Nanomed. Nanotech. 7, 1–4.
Ibrahim, H.M., 2015. Green synthesis and characterization of silver nanoparticles using banana peel extract and their antimicrobial activity against representative microorganisms. J. Radiat. Res. Appl. Sci. 8, 265–275.
Ingham, B., 2015. X-ray scattering characterisation of nanoparticles. Crystallogr. Rev. 21, 229–303.
Iravani, S., 2011. Green synthesis of metal nanoparticles using plants. Green Chem. 13, 2638–2650.
Iravani, S., Korbekandi, H., Mirmohammadi, S.V., Zolfaghari, B., 2014. Synthesis of silver nanoparticles: chemical, physical and biological methods. Res Pharm. Sci. 9, 385–406.
Jeffryes, C., Agathos, S.N., Rorrer, G., 2015. Biogenic nanomaterials from photosynthetic microorganisms. Curr. Opin. Biotechnol. 33, 23–31.
Jena, J., Pradhan, N., Dash, B.P., Sukla, L.B., Panda, P.K., 2013. Biosynthesis and characterization of silver nanoparticles using microalga *Chlorococcum humicola* and its antibacterial activity. Int. J. Nanomater. Biostruct. 3, 1–8.
Jena, J., Pradhan, N., Nayak, R.R., Dash, B.P., Sukla, L.B., Panda, P.K., Mishra, B.K., 2014. Microalga *Scenedesmus* sp.: a potential low-cost green machine for silver nanoparticle synthesis. J. Microbiol. Biotechnol. 24, 522–533.
Jena, J., Pradhan, N., Aishvarya, V., Nayak, R.R., Dash, B.P., Sukla, L.B., Panda, P.K., Mishra, B.K., 2015. Biological sequestration and retention of cadmium as CdS nanoparticles by the microalga *Scenedesmus*-24. J. Appl. Phycol. 27, 2251–2260.
Kalabegishvili, T.L., Kirkesali, E.I., Rcheulishvili, A.N., Ginturi, E.N., Murusidze, I.G., Pataraya, D.T., Gurielidze, M.A., Tsertsvadze, G.I., Gabunia, V.N., Lomidze, L.G., Gvarjaladze, D.N., 2012. Synthesis of gold nanoparticles by some strains of *Arthrobacter* genera. Proc. Inst. Mech. Eng. Part L J. Mat. Des. Appl. 7, 1–7.
Kanimozhi, S., Johnson, A., Kala, M., Shibila, P.C., Revathy, I., 2015. Extracellular synthesis of silver nanoparticles from a marine alga, *Sargassum polycystum* C. Agardh and their biopotentials. World J. Pharm. Pharm. Sci. 4, 1388–1400.
Kannan, R.R.R., Arumugam, R., Ramya, D., Manivannan, K., Anantharaman, P., 2013a. Green synthesis of silver nanoparticles using marine macroalga *Chaetomorpha linum*. Appl. Nanosci. 3, 229–233.
Kannan, R.R.R., Stirk, W.A., Van Staden, J., 2013b. Synthesis of silver nanoparticles using the seaweed *Codium capitatum* P.C. Silva (Chlorophyceae). S. Afr. J. Bot. 86, 1–4.
Karthikeyan, P., Mohan, D., Abishek, G., Priya, R., 2015. Synthesis of silver nanoparticles using Phytoplankton and its characteristics. Int. J. Fish Aquac. Stu. 2, 398–401.
Kathiraven, T., Sundaramanickam, A., Shanmugam, N., Balasubramanian, T., 2015. Green synthesis of silver nanoparticles using marine algae *Caulerpa racemosa* and their antibacterial activity against some human pathogens. Appl. Nanosci. 5, 499–504.
Keat, C.L., Aziz, A., Eid, A.M., Elmarzugi, N.A., 2015. Biosynthesis of nanoparticles and silver nanoparticles. Bioresour. Bioprocess 2, 47.
Khalil, M.M., Ismail, E.H., El-Baghdady, K.Z., Mohamed, D., 2014. Green synthesis of silver nanoparticles using olive leaf extract and its antibacterial activity. Arab. J. Chem. 7, 1131–1139.
Khan, I., Saeed, K., Khan, I., 2017. Nanoparticles: properties, applications and toxicities. Arab. J. Chem. https://doi.org/10.1016/j.arabjc.2017.05.011.
Krishnan, M., Sivanandham, V., Hans-Uwe, D., Murugaiah, S.G., Seeni, P., Gopalan, S., Rathinam, A.J., 2015. Antifouling assessments on biogenic nanoparticles: a field study from polluted offshore platform. Mar. Pollut. Bull. 101, 816–825.
Kumar, P., Selvi, S.S., Praba, A.L., Selvaraj, M., 2012a. Antibacterial activity and in-vitro cytotoxicity assay against brine shrimp using silver nanoparticles synthesized from *Sargassum ilicifolium*. Dig. J. Nanomater Biostruct. 7, 1447–1455.
Kumar, P., Senthamilselvi, S., Lakshmipraba, A., Premkumar, K., Muthukumaran, R., Visvanathan, P., Ganeshkumar, R.S., Govindaraju, M., 2012b. Efficacy of bio-synthesized silver nanoparticles using *Acanthophora spicifera* to encumber biofilm formation. Dig. J. Nanomater Biostruct. 7, 511–522.
Kumar, P., Govindaraju, M., Senthamilselvi, S., Premkumar, K., 2013a. Photocatalytic degradation of methyl orange dye using silver (Ag) nanoparticles synthesized from *Ulva lactuca*. Colloids Surf. B: Biointerfaces 103, 658–661.
Kumar, P., Selvi, S.S., Govindaraju, M., 2013b. Seaweed-mediated biosynthesis of silver nanoparticles using *Gracilaria corticata* for its antifungal activity against *Candida* spp. Appl. Nanosci. 3, 495–500.

Lellouche, J., Kahana, E., Elias, S., Gedanken, A., Banin, E., 2009. Antibiofilm activity of nanosized magnesium fluoride. Biomaterials 30 (30), 5969–5978.
Lengke, M.F., Fleet, M.E., Southam, G., 2006a. Morphology of gold nanoparticles synthesized by filamentous cyanobacteria from gold(I)-thiosulfate and gold(III)–chloride complexes. Langmuir. 22, 2780–2787.
Lengke, M.F., Fleet, M.E., Southam, G., 2006b. Synthesis of platinum nanoparticles by reaction of filamentous cyanobacteria with platinum (IV)-chloride complex. Langmuir. 22, 7318–7323.
Lengke, M.F., Ravel, B., Fleet, M.E., Wanger, G., 2006c. Mechanisms of gold bioaccumulation by filamentous cyanobacteria from gold (III)− chloride complex. Sci. Technol. China 40, 6304–6309.
Lengke, M.F., Fleet, M.E., Southam, G., 2007a. Biosynthesis of silver nanoparticles by filamentous cyanobacteria from a silver(I) nitrate complex. Langmuir. 23, 2694–2699.
Lengke, M.F., Fleet, M.E., Southam, G., 2007b. Synthesis of palladium nanoparticles by reaction of filamentous cyanobacterial biomass with a palladium(II) chloride complex. Langmuir. 23, 8982–8987.
LewisOscar, F., Vismaya, S., Arunkumar, M., Thajuddin, N., Dhanasekaran, D., Nithya, C., 2016. Algal nanoparticles: synthesis and biotechnological potentials. In: Algae-Organisms for Imminent Biotechnology. IntechOpen.
Li, X., Xu, H., Chen, Z.S., Chen, G., 2011. Biosynthesis of nanoparticles by microorganisms and their applications. J. Nanomater. 2011, 1–16.
Li, X., Schirmer, K., Bernard, L., Sigg, L., Pillai, S., Behra, R., 2015a. Silver nanoparticle toxicity and association with the alga *Euglena gracilis*. Environment. Sci. Nano. 2, 594–602.
Li, Y., Tang, X., Song, W., Zhu, L., Liu, X., Yan, X., Jin, C., Ren, Q., 2015b. Biosynthesis of silver nanoparticles using *Euglena gracilis, Euglena intermedia and their extract*. IET Nanobiotechnol. 9, 19–26.
Liu, B., Xie, J., Lee, J.Y., Ting, Y.P., Chen, J.P., 2005. Optimization of high-yield biological synthesis of single-crystalline gold nanoplates. J. Phys. Chem. B 109, 15256–15263.
Luangpipat, T., Beattie, I.R., Chisti, Y., Haverkamp, R.G., 2011. Gold nanoparticles produced in a microalga. J. Nanopart. Res. 13, 6439–6445.
Madhiyazhagan, P., Murugan, K., Kumar, A.N., Nataraj, T., Dinesh, D., Panneerselvam, C., Subramaniam, J., Kumar, P.M., Suresh, U., Roni, M., Nicoletti, M., 2015. *Sargassum muticum*-synthesized silver nanoparticles: an effective control tool against mosquito vectors and bacterial pathogens. Parasitol. Res. 114 (11), 4305–4317.
Mahdavi, M., Namvar, F., Ahmad, M.B., Mohamad, R., 2013. Green biosynthesis and characterization of magnetic iron oxide (Fe_3O_4) nanoparticles using seaweed (*Sargassum muticum*) aqueous extract. Molecules. 18, 5954–5964.
Mahdieh, M., Zolanvari, A., Azimee, A.S., Mahdieh, M., 2012. Green biosynthesis of silver nanoparticles by *Spirulina platensis*. Scientia Iranica. 19, 926–929.
Makarov, V.V., Love, A.J., Sinitsyna, O.V., 2014. "Green" nanotechnologies: synthesis of metal nanoparticles using plants. Acta Nat. 6, 35–44.
Mata, Y.N., Torres, E., Blazquez, M.L., Ballester, A., González, F.M.J.A., Munoz, J.A., 2009. Gold (III) biosorption and bioreduction with the brown alga *Fucus vesiculosus*. J. Hazard. Mater. 166, 612–618.
Menon, S., Rajeshkumar, S., Kumar, V., 2017. A review on biogenic synthesis of gold nanoparticles, characterization, and its applications. Resource-Efficient Technol. 3 (4), 516–527.
Michalak, I., Chojnacka, K., 2015. Algae as production systems of bioactive compounds. Eng. Life Sci. 15, 160–176.
Mohandass, C., Vijayaraj, A.S., Rajasabapathy, R., Satheeshbabu, S., Rao, S.V., Shiva, C., De-Mello, I., 2013. biosynthesis of silver nanoparticles from marine seaweed *Sargassum cinereum* and their antibacterial activity. J. Invest Dermatol. 78, 206–209.
Mohseniazar, M., Barin, M., Zarredar, H., Alizadeh, S., Shanehbandi, D., 2011. Potential of microalgae and *lactobacilli* in biosynthesis of silver nanoparticles. Bioimpacts. 1, 149–152.
Momeni, S., Nabipour, I., 2015. A simple green synthesis of palladium nanoparticles with Sargassum alga and their electrocatalytic activities towards hydrogen peroxide. App. Biochem. Biotechnol. 176 (7), 1937–1949.
MubarakAli, D., Gopinath, V., Rameshbabu, N., Thajuddin, N., 2012. Synthesis and characterization of CdS nanoparticles using C-phycoerythrin from the marine cyanobacteria. Mater. Lett. 74, 8–11.
MubarakAli, D., Arunkumar, J., Nag, K.H., SheikSyedIshack, K.A., Baldev, E., Pandiaraj, D., Thajuddin, N., 2013. Gold nanoparticles from Pro and eukaryotic photosynthetic microorganisms-Comparative studies on synthesis and its application on biolabelling. Colloid Surfaces B 103, 166–173.
Mukherjee, P., Senapati, S., Mandal, D., Ahmad, A., Khan, M.I., Kumar, R., Sastry, M., 2002. Extracellular synthesis of gold nanoparticles by the fungus *Fusarium oxysporum*. Chembiochem. 3, 461–463.
Mukherji, S., Ruparelia, J., Agnihotri, S., 2012. Antimicrobial activity of silver and copper nanoparticles: variation in sensitivity across various strains of bacteria and fungi. Nano-antimicrobials. 225–251.
Murugan, K., Samidoss, C.M., Panneerselvam, C., Higuchi, A., Roni, M., Suresh, U., Chandramohan, B., Subramaniam, J., Madhiyazhagan, P., Dinesh, D., Rajaganesh, R., 2015. Seaweed-synthesized silver nanoparticles: an eco-friendly tool in the fight against *Plasmodium falciparum* and its vector *Anopheles stephensi*? Parasitol. Res. 114, 4087–4097.
Murugesan, S., Elumalai, M., Dhamotharan, R., 2011. Green synthesis of silver nano particles from marine alga *Gracilaria edulis*. Biosci. Biotech. Res. Comm. 4, 105–110.
Nagarajan, S., Arumugam, Kuppusamy K., 2013. Extracellular synthesis of zinc oxide nanoparticle using seaweeds of gulf of Mannar, India. J. Nanobiotechnol. 11, 39.
Namvar, F., Azizi, S., Ahmad, M.B., Shameli, K., Mohamad, R., Mahdavi, M., Tahir, P.M., 2015. Green synthesis and characterization of gold nanoparticles using the marine macroalgae *Sargassum muticum*. Res. Chem. Intermed. 41, 5723–5730.
Nath, D., Banerjee, P., 2013. Green nanotechnology–a new hope for medical biology. Environ. Toxicol. Pharmacol. 36, 997–1104.
Naveena, B.E., Prakash, S., 2013. Biological synthesis of gold nanoparticles using marine algae *Gracilaria corticata* and its application as a potent antimicrobial and antioxidant agent. Asian J. Pharm. Clin. Res. 6, 179–182.
Oza, G., Pandey, S., Mewada, A., Kalita, G., Sharon, M., Phata, J., Ambernath, W., Sharon, M., 2012. Facile biosynthesis of gold nanoparticles exploiting optimum pH and temperature of fresh water algae *Chlorella pyrenoidusa*. Adv. Appl. Sci. Res. 3, 1405.
Parial, D., Pal, R., 2014. Green synthesis of gold nanoparticles using cyanobacteria and their characterization. Indian J. Appl. Res. 4, 69–72.
Parial, D., Pal, R., 2015. Biosynthesis of monodisperse gold nanoparticles by green alga *Rhizoclonium* and associated biochemical changes. J. Appl. Phycol. 27, 975–984.
Parial, D., Patra, H.K., Dasgupta, A.K.R., Pal, R., 2012a. Screening of different algae for green synthesis of gold nanoparticles. Eur. J. Phycol. 47, 22–29.
Parial, D., Patra, H.K., Roychoudhury, P., Dasgupta, A.K., Pal, R., 2012b. Gold nanorod production by cyanobacteria—a green chemistry approach. J. Appl. Phycol. 24, 55–60.
Patel, V., Berthold, D., Puranik, P., Gantar, M., 2015. Screening of cyanobacteria and microalgae for their ability to synthesize silver nanoparticles with antibacterial activity. Biotechnol. Rep. 5, 112–119.
Pathak, J., Ahmed, H., Singh, D.K., Pandey, A., Singh, S.P., Sinha, R.P., 2019. Recent developments in green synthesis of metal nanoparticles utilizing cyanobacterial cell factories. In: Nanomaterials in Plants, Algae and Microorganisms. Academic Press, pp. 237–265.
Pinjarkar, H., Gaikwad, S., Ingle, A.P., Gade, A., Rai, M., 2016. Phycofabrication of silver nanoparticles and their antibacterial activity against human pathogens. Adv. Mater. Lett. 7, 1010–1014.
Poinern, G.E.J., 2014. A Laboratory Course in Nanoscience and Nanotechnology. CRC Press.
Prasad, T.N.V.K.V., Elumalai, E.K., 2013. Marine algae mediated synthesis of silver nanopaticles using *Scaberia agardhii Greville*. J. Biol. Sci. 13, 566–569.
Prasad, B., Padmesh, T., 2014. Seaweed (*Sargassum ilicifolium*) assisted green synthesis of palladium nanoparticles. Int. J. Sci. Eng. Res. 5, 229–231.
Prasad, T.N.V.K.V., Kambala, V.S.R., Naidu, R., 2013. Phyconanotechnology: synthesis of silver nanoparticles using brown marine algae *Cystophora moniliformis* and their characterisation. J. Appl. Phycol. 25, 177–182.
Prasad, R., Pandey, R., Barman, I., 2016. Engineering tailored nanoparticles with microbes: quo vadis? Wiley Interdiscip. Rev. Nanomed. Nanobiotechnol. 8 (2), 316–330.
Priyadharshini, R.I., Prasannaraj, G., Geetha, N., 2014. Microwave-mediated extracellular synthesis of metallic silver and zinc oxide nanoparticles using macro-algae (*Gracilaria edulis*) extracts and its anticancer activity against human PC3 cell lines. Appl. Biochem. Biotechnol. 174, 2777–2790.
Quester, K., Avalos-Borja, M., Castro-Longoria, E., 2013. Biosynthesis and microscopic study of metallic nanoparticles. Micron 54, 1–27.
Rahdar, A., 2013. Study of different capping agent effect on the structural and optical properties of Mn doped ZnS nanostructures. World Appl. Programm. 3, 56–60.
Rahimi, Z., Yousefzadi, M., Noori, A., 2014. Green synthesis of silver nanoparticles using *Ulva flexousa* from the Persian Gulf, Iran. J. Persian Gulf. 5, 9–16.
Rahman, A., Ismail, A., Jumbianti, D., Magdalena, S., Sudrajat, H., 2009. Synthesis of copper oxide nano particles by using *Phormidium cyanobacterium*. Indones J. Chem. 9, 355–360.
Rajasulochana, P., Krishnamoorthy, P., Dhamotharan, R., 2012. Potential application of *Kappaphycus alvarezii* in agricultural and pharmaceutical industry. J. Chem. Pharm. Res. 4, 33–37.
Rajathi, A.A.F., Parthiban, C., Kumar, V.G., Anantharaman, P., 2012. Biosynthesis of antibacterial gold nanoparticles using brown alga, *Stoechospermum marginatum* (kützing). Spectrochim. Acta A Mol. Biomol. Spectrosc. 99, 166–173.
Rajesh, S., Raja, D.P., Rathi, J.M., Sahayaraj, K., 2012. Biosynthesis of silver nanoparticles using *Ulva fasciata* (Delile) ethyl acetate extract and its activity against *Xanthomonas campestris* pv. *malvacearum*. J. Biopest. 5, 119–128.
Rajeshkumar, S., Kannan, C., Annadurai, G., 2012a. Green synthesis of silver nanoparticles using marine brown algae *Turbinaria conoides* and its antibacterial activity. Int. J. Pharm. Bio Sci. 3, 502–510.
Rajeshkumar, S., Kannan, C., Annadurai, G., 2012b. Synthesis and characterization of antimicrobial silver nanoparticles using marine brown seaweed *Padina tetrastromatica*. Drug Invent. Today 4, 511–513.
Rajeshkumar, S., Malarkodi, C., Gnanajobitha, G., Paulkumar, K., Vanaja, M., Kannan, C., Annadurai, G., 2013a. Seaweed-mediated synthesis of gold nanoparticles using *Turbinaria conoides* and its characterization. J. Nanostruct. Chem. 3, 44.
Rajeshkumar, S., Malarkodi, C., Vanaja, M., Gnanajobitha, G., Paulkumar, K., Kannan, C., Annadurai, G., 2013b. Antibacterial activity of algae mediated synthesis of gold nanoparticles from *Turbinaria conoides*. Der. Pharma Chem. 5, 224–229.
Rajeshkumar, S., Malarkodi, C., Paulkumar, K., Vanaja, M., Gnanajobitha, G., Annadurai, G., 2014. Algae mediated green fabrication of silver nanoparticles and examination of its antifungal activity against clinical pathogens. Int. J. Met. 2014, 1–8.
Ramakrishna, M., Babu, D.R., Gengan, R.M., Chandra, S., Rao, G.N., 2016. Green synthesis of gold nanoparticles using marine algae and evaluation of their catalytic activity. J. Nanostruct. Chem. 6, 1–13.
Ramakritinan, C.M., Kaarunya, E., Shankar, S., Kumaraguru, A.K., 2013. Antibacterial effects of Ag, Au and bimetallic (Ag-Au) nanoparticles synthesized from red algae. In: Solid State Phenomena. 201. Trans Tech Publications, pp. 211–230.
Roe, D., Karandikar, B., Bonn-Savage, N., Gibbins, B., Roullet, J.B., 2008. Antimicrobial surface functionalization of plastic catheters by silver nanoparticles. J. Antimicrob. Chemother. 61 (4), 869–876.
Rösken, L.M., Cappel, F., Körsten, S., Fischer, C.B., Schönleber, A., van Smaalen, S.,

Geimer, S., Beresko, C., Ankerhold, G., Wehner, S., 2016. Time-dependent growth of crystalline Au0-nanoparticles in cyanobacteria as self-reproducing bioreactors: 2. *Anabaena cylindrica*. Beilstein J. Nanotechnol. 7 (1), 312–327.
Roychoudhury, P., Pal, R., 2014. *Spirogyra submaxima*–a green alga for nanogold production. J. Algal Biomass Utln. 5, 15–19.
Sahayaraj, K., Rajesh, S., Rathi, J.M., 2012. Silver nanoparticles biosynthesis using marine alga *Padina pavonica* (linn.) and its microbicidal activity. Dig. J. Nanomater Biostruct. 7, 1557–1567.
Sahoo, P.C., Kausar, F., Lee, J.H., Han, J.I., 2014. Facile fabrication of silver nanoparticle embedded $CaCO_3$ microspheres via microalgae-templated CO_2 biomineralization: application in antimicrobial paint application. RSC Adv. 4, 32562–32569.
Sajidha, Parveen K., Lakshmi, D., 2016. Biosynthesis of silver nanoparticles using red algae, *Amphiroa fragilissima* and its antibacterial potential against Gram positive and Gram negative bacteria. Int. J. Curr. Sci. 19, 93–100.
Salari, Z., Danafar, F., Dabaghi, S., Ataei, S.A., 2016. Sustainable synthesis of silver nanoparticles using macroalgae *Spirogyra varians* and analysis of their antibacterial activity. J Saudi Chem. Soc. 20, 459–464.
Sanaeimehr, Z., Javadi, I., Namvar, F., 2018. Antiangiogenic and antiapoptotic effects of green-synthesized zinc oxide nanoparticles using *Sargassum muticum* algae extraction. Cancer Nanotechnol. 9 (1), 3.
Sangeetha, N., Saravanan, K., 2014. Biogenic silver nanoparticles using marine seaweed (*Ulva lactuca*) and evaluation of its antibacterial activity. J. Nanosci. Nanotechnol. 2, 99–102.
Sangeetha, G., Rajeshwari, S., Venckatesh, R., 2011. Green synthesis of zinc oxide nanoparticles by *aloe barbadensis* miller leaf extract: Structure and optical properties. Mater. Res. Bull. 46 (12), 2560–2566.
Sastry, M., Ahmad, A., Khan, M.I., Kumar, R., 2003. Biosynthesis of metal nanoparticles using fungi and actinomycete. Curr. Sci. 85, 162–170.
Satapathy, S., Shukla, S.P., Sandeep, K.P., Singh, A.R., Sharma, N., 2015. Evaluation of the performance of an algal bioreactor for silver nanoparticle production. J. Appl. Phycol. 27, 285–291.
Schröfel, A., Kratošová, G., Bohunická, M., Dobročka, E., Vávra, I., 2011. Biosynthesis of gold nanoparticles using diatoms—silica-gold and EPS-gold bionanocomposite formation. J. Nanopart. Res. 13, 3207–3216.
Sekine, N., Chou, C.-H., Kwan, W.L., Yang, Y., 2009. ZnO nano-ridge structure and its application in inverted polymer solar cell. Org. Electron. 10, 1473–1477.
Senapati, S., Syed, A., Moeez, S., Kumar, A., Ahmad, A., 2012. Intracellular synthesis of gold nanoparticles using alga *Tetraselmis kochinensis*. Mater. Lett. 79, 116–118.
Shabnam, N., Pardha-Saradhi, P., 2013. Photosynthetic electron transport system promotes synthesis of Au-nanoparticles. PLoS One 8, e71123.
Shah, M., Fawcett, D., Sharma, S., Tripathy, S., Poinern, G., 2015. Green synthesis of metallic nanoparticles via biological entities. Materials. 8, 7278–7308.
Shakibaie, M., Forootanfar, H., Mollazadeh-Moghaddam, K., Bagherzadeh, Z., Nafissi-Varcheh, N., Shahverdi, A.R., Faramarzi, M.A., 2010. Green synthesis of gold nanoparticles by the marine microalga *Tetraselmis suecica*. Biotechnol. Appl. Biochem. 57, 71–75.
Sharma, D., Sharma, S., Kaith, B.S., Rajput, J., Kaur, M., 2011. Synthesis of ZnO nanoparticles using surfactant free in-air and microwave method. Appl. Surf. Sci. 257, 9661–9672.
Sharma, B., Purkayastha, D.D., Hazra, S., Gogoi, L., Bhattacharjee, C.R., Ghosh, N.N., Rout, J., 2014a. Biosynthesis of gold nanoparticles using a freshwater green alga, *Prasiola crispa*. Mater Lett. 116, 94–97.
Sharma, B., Purkayastha, D.D., Hazra, S., 2014b. Biosynthesis of fluorescent gold nanoparticles using an edible freshwater red alga, *Lemanea fluviatilis* (L.) C. Ag. and antioxidant activity of biomatrix loaded nanoparticles. Bioprocess Biosyst. Eng. 37, 2559–2565.
Sharma, D., Kanchi, S., Bisetty, K., 2015a. Biogenice synthesis of nanoparticles: a review. Arab. J. Chem. https://doi.org/10.1016/j.arabjc.2015.11.002.
Sharma, G., Jasuja, N.D., Kumar, M., Ali, M.I., 2015b. Biological Synthesis of Silver Nanoparticles by Cell-Free Extract of *Spirulina platensis*. J. Nanotechnol. 2015. https://doi.org/10.1155/2015/132675.
Sharma, A., Sharma, S., Sharma, K., Chetri, S.P., Vashishtha, A., Singh, P., Kumar, R., Rathi, B., Agrawal, V., 2016. Algae as crucial organisms in advancing nanotechnology: a systematic review. J. Appl. Phycol. 28, 1759–1774.
Shedbalkar, U., Singh, R., Wadhwani, S., Gaidhani, S., Chopade, B.A., 2014. Microbial synthesis of gold nanoparticles: current status and future prospects. Adv. Colloid Interf. Sci. 209, 40–48.
Shiny, P.J., Mukherjee, A., Chandrasekaran, N., 2013. Marine algae mediated synthesis of the silver nanoparticles and its antibacterial efficiency. Int J Pharm Pharm Sci 5, 239–241.
Shukla, A.K., Iravani, S., 2017. Metallic nanoparticles: green synthesis and spectroscopic characterization. Environ. Chem. Lett. 15 (2), 223–231.
Shukla, M.K., Singh, R.P., Reddy, C.R.K., Jha, B., 2012. Synthesis and characterization of agar-based silver nanoparticles and nanocomposite film with antibacterial applications. Bioresour. Technol. 107, 295–300.
Sicard, C., Brayner, R., Margueritat, J., Hémadi, M., Couté, A., Yéprémian, C., Djediat, C., Aubard, J., Fiévet, F., Livage, J., Coradin, T., 2010. Nano- gold biosynthesis by silica -encapsulated micro-algae: a "living" bio-hybrid material. J. Mater. Chem. 20, 9342–9347.
Siddiqui, M.N., Redhwi, H.H., Achilias, D.S., Kosmidou, E., Vakalopoulou, E., Ioannidou, M.D., 2017. Green synthesis of silver nanoparticles and study of their antimicrobial properties. J. Polym. Environ. 1–11.
Singaravelu, G., Arockiamary, J.S., Kumar, V.G., Govindaraju, K., 2007. A novel extracellular synthesis of monodisperse gold nanoparticles using marine alga, *Sargassum wightii Greville*. Colloids Surf. B: Biointerfaces 57, 97–101.
Singh, M., Kalaivani, R., Manikandan, S., Sangeetha, N., Kumaraguru, A.K., 2013. Facile green synthesis of variable metallic gold nanoparticle using *Padina gymnospora*, a brown marine macroalga. Appl. Nanosci. 3, 145–151.
Singh, G., Babele, P.K., Kumar, A., Srivastava, A., Sinha, R.P., Tyagi, M.B., 2014a. Synthesis of ZnO nanoparticles using the cell extract of the cyanobacterium, *Anabaena* strain L31 and its conjugation with UV-B absorbing compound shinorine. J. Photochem. Photobiol. B 138, 55–62.
Singh, M., Kumar, M., Manikandan, S., Chandrasekaran, N., Mukherjee, A., Kumaraguru, A.K., 2014b. Drug delivery system for controlled cancer therapy using physico-chemically stabilized bioconjugated gold nanoparticles synthesized from marine macroalgae, *Padina Gymnospora*. J. Nanomed. Nanotechol. S5, 1–7.
Sinha, S., Pan, I., Chanda, P., Sen, S.K., 2009. Nanoparticles fabrication using ambient biological resources. J. Appl. Biosci. 19, 1113–1130.
Sinha, S.N., Paul, D., Halder, N., Sengupta, D., Patra, S.K., 2015. Green synthesis of silver nanoparticles using fresh water green alga *Pithophora oedogonia* (Mont.) Wittrock and evaluation of their antibacterial activity. Appl. Nanosci. 5, 703–709.
Subramaniyam, V., Subashchandrabose, S.R., Thavamani, P., Megharaj, M., Chen, Z., Naidu, R., 2015. *Chlorococcum* sp. MM11—a novel phyco-nanofactory for the synthesis of iron nanoparticles. J. Appl. Phycol. 27, 1861–1869.
Sudha, S.S., Amanickam, K., Rengaramanujam, J., 2013. Microalgae mediated synthesis of silver nanoparticles and their antibacterial activity against pathogenic bacteria. Indian J. Exp. Biol. 51, 393–399.
Suganya, K.U., Govindaraju, K., Kumar, V.G., Dhas, T.S., Karthick, V., Singaravelu, G., Elanchezhiyan, M., 2015. Blue green alga mediated synthesis of gold nanoparticles and its antibacterial efficacy against Gram positive organisms. Mater. Sci. Eng. C 47, 351–356.
Suriya, J., Bharathi Raja, S., Sekar, V., Rajasekaran, R., 2012. Biosynthesis of silver nanoparticles and its antibacterial activity using seaweed *Urospora* sp. Afr. J. Biotechnol. 11, 12192–12198.
Tanaka, Y., 2018. Synthesis of nanosize particles in thermal plasmas. In: Handbook of Thermal Science and Engineering, pp. 2791–2828.
Thakkar, K.N., Mhatre, S.S., Parikh, R.Y., 2010. Biological synthesis of metallic nanoparticles. Nanomedicine. 6, 257–262.
Thangaraju, N., Venkatalakshmi, R.P., Chinnasamy, A., Kannaiyan, P., 2012. Synthesis of silver nanoparticles and the antibacterial and anticancer activities of the crude extract of *Sargassum polycystum* C. Agardh Nano Biomed. Eng. 4, 89–94.
Ting, Y.P., Teo, W.K., Soh, C.Y., 1995. Gold uptake by *Chlorella vulgaris*. J. Appl. Phycol. 7, 97–100.
Tsibakhashvili, N.Y., Kirkesali, E.I., Pataraya, D.T., Gurielidze, M.A., Kalabegishvili, T.L., Gvarjaladze, D.N., Tsertsvadze, G.I., Frontasyeva, M.V., Zinicovscaia, I.I., Wakstein, M.S., Khakhanov, S.N., 2011. Microbial synthesis of silver nanoparticles by *Streptomyces glaucus* and *Spirulina platensis*. Adv. Sci. Lett. 4, 1–10.
Türk, M., Erkey, C., 2018. Synthesis of supported nanoparticles in supercritical fluids by supercritical fluid reactive deposition: current state, further perspectives and needs. J. Supercrit Fluids 134, 176–183.
Ullah, H., Khan, I., Yamani, Z.H., Qurashi, A., 2017. Sonochemical-driven ultrafast facile synthesis of SnO_2nanoparticles: growth mechanism structural electrical and hydrogen gas sensing proper-ties. Ultrason. Sonochem. 34, 484–490.
Varun, S., Sudha, S., Kumar, P.S., 2014. Biosynthesis of gold nanoparticles from aqueous extract of *Dictyota Bartayresiana* and their antifungal activity. Indian J. Adv. Chem. Sci. 2, 190–193.
Velammal, S.P., Devi, T.A., Amaladhas, T.P., 2016. Antioxidant, antimicrobial and cytotoxic activities of silver and gold nanoparticles synthesized using *Plumbago zeylanica* bark. J. Nanostructure Chem. 6, 247–260.
Venkatesan, J., Manivasagan, P., Kim, S.K., Kirthi, A.V., Marimuthu, S., Rahuman, A.A., 2014. Marine algae-mediated synthesis of gold nanoparticles using a novel *Ecklonia cava*. Bioprocess Biosyst. Eng. 37, 1591–1597.
Verma, V.C., Kharwar, R.N., Gange, A.C., 2010. Biosynthesis of antimicrobial silver nanoparticles by the endophytic fungus *Aspergillus clavatus*. Nanomedicine. 5, 33–40.
Vijayan, S.R., Santhiyagu, P., Singamuthu, M., Kumari Ahila, N., Jayaraman, R., Ethiraj, K., 2014. Synthesis and characterization of silver and gold nanoparticles using aqueous extract of seaweed, *Turbinaria conoides*, and their antimicrofouling activity. Sci. World J. 2014, 938272.
Vijayan, S.R., Santhiyagu, P., Ramasamy, R., Arivalagan, P., Kumar, G., Ethiraj, K., Ramaswamy, B.R., 2016. Seaweeds: a resource for marine bionanotechnology. Enzym. Microb. Technol. 95, 45–57.
Vijayaraghavan, K., Mahadevan, A., Sathishkumar, M., Pavagadhi, S., Balasubramanian, R., 2011. Biosynthesis of Au (0) from Au (III) via biosorption and bioreduction using brown marine alga *Turbinaria conoides*. Chem. Eng. J. 167 (1), 223–227.
Vivek, M., Kumar, P.S., Steffi, S., Sudha, S., 2011. Biogenic silver nanoparticles by *Gelidiella acerosa* extract and their antifungal effects. Avicenna J. Med. Biotechnol. 3, 143–148.
Xie, J., Lee, J.Y., Wang, D.I.C., Ting, Y.P., 2007a. Silver nanoplates: from biological to biomimetic synthesis. ACS Nano 1, 429–439.
Xie, J., Lee, J.Y., Wang, D., Ting, Y.P., 2007b. Identification of active biomolecules in the high-yield synthesis of single-crystalline gold nanoplates in algal solutions. Small. 3, 672–682.
Yousefzadi, M., Rahimi, Z., Ghafori, V., 2014. The green synthesis, characterization and antimicrobial activities of silver nanoparticles synthesized from green alga *Enteromorpha flexuosa* (wulfen) J. Agardh. Mater Lett. 137, 1–4.
Zinicovscaia, I., 2012. Use of bacteria and microalgae in synthesis of nanoparticles. Chem. J. Mold. 7, 32–38.